The Actin Regulatory Protein Hem1 Regulates T cell Homeostasis and Cytokine Production in a T Cell Specific Manner

Alexandra Christodoulou

A thesis

submitted in partial fulfillment of the

requirements for the degree of

Master of Science

University of Washington

2023

Committee:

Brian Iritani

Thea Brabb

Charles Frevert

Michael Gerner

Program Authorized to Offer Degree:

Comparative Medicine

University of Washington

Abstract

The Actin Regulatory Protein Hem1 Regulates T Cell Homeostasis and Cytokine Production in a T Cell Specific Manner

Alexandra Christodoulou

Chair of the Supervisory Committee:

Brian Iritani

Department of Comparative Medicine

Hematopoietic Protein-1 (Hem1) is a hematopoietic cell specific component of the actin regulatory WAVE complex, which is activated downstream of multiple immune receptors and a mediator of f-actin polymerization. Mutations in the *NCKAP1L* gene encoding HEM1 have recently been found to result in severe Primary Immunodeficiency Disease (PID) in children. We utilized mouse models of constitutive and conditional deletion of *Nckap1l* to study the role Hem1 plays in T cell development, activation, and function. Hem1 deficient T cells exhibit ed a shift towards decreased naïve and increased memory T cells, and increased frequency of regulatory T cells. Loss of Hem1 specifically in T cells resulted in hallmarks of CD4 T cell exhaustion, including CD4 T cell lymphopenia, decreased activation and proliferation, increased expression of the inhibitory receptors PD-1 and Tim3, and increased IL-10 production. *In vitro* TCR stimulation of CD4 T cells resulted in significantly decreased expression of IL-2, and significantly increased production of the Th2 cytokines IL-4, IL-5, IL-13; increased Th17 cytokines IL-17, IL-22; and increased Treg

cytokine IL-10. This correlated with decreased F-actin capping and increased expression of CD107a indicative of increased granule membrane fusion, suggesting increased release of cytokines secondary to cortical actin disruption. These results collectively suggest that Hem-1 and the WAVE Regulatory Complex (WRC) are critical for maintaining CD4 T cell homeostasis and regulated cytokine production following T cell activation.

TABLE OF CONTENTS

Introduction……..…1

Materials and Methods……..…….....3

Results…….....7

Discussion……15

Figures…….20

References……33

INTRODUCTION

Hematopoietic protein 1 (Hem-1) is a hematopoietic cell-specific component of the WASP Family Verprolin homologous protein (WAVE) regulatory complex (WRC) which activates filamentous actin (f-actin) polymerization downstream of immune-receptor signaling (Park *et. al*, 2010). Hem1 interacts with Rac and WAVE proteins to activate the Arp2/3 complex-mediated f-actin polymerization (Park *et al.*, 2010; Dupre *et al*., 2021) . F-actin polymerization plays an essential role in immune cellular processes, including phagocytosis, synapse formation, lamellipodia formation and cell migration, and regulated exocytosis (Cook *et al.,* 2020; Park *et al.*, 2010). F-actin also participates in cell spreading and immune synapse formation, affecting immune cell receptor and antigen recognition and downstream lymphocyte activation (Cook *et al.*, 2022; Dupre *et al.,* 2021). Branched f-actin also forms lamellipodia at the cell membrane surface which are essential for lymphocyte migration to the periphery. In addition, a dense ring of branched actin lies underneath the cell membrane at the periphery of the cytoplasm, creating a cortical actin barrier that helps regulate vesicle secretion (Cook *et al*., 2022). Impaired f-actin polymerization can lead to disruptions in the cortical actin barrier, resulting in unregulated release of cytokines and degranulation (Cook *et al.,* 2022). Recently, reports describing patients with loss-of-function mutations in the *NCKAP1L (Hem1)* gene have shown how improper actin polymerization and networks secondary to Hem1 deficiency can lead to a clinical syndrome with recurrent infections and autoimmunity (Cook *et al.*, 2020; Castro *et al.*, 2020; Salzer *et. al*, 2020).

Nine pediatric patients from seven different lineages have recently been identified with primary immune disorders (PID) secondary to loss-of-function mutations in the *NCKAP1L* gene encoding the Hem-1 protein (Cook *et al.*, 2020; Castro *et al.*, 2020; Salzer *et. al*, 2020). The clinical picture in the patients identified so far varies, however most suffer from recurrent infections and hyperinflammation resulting in a high mortality rate at a young age. In addition to immunodeficiency, more than half of the patients identified exhibit atopic or autoimmune diseases and some patients had disease involving hyperinflammation and lymphoproliferation similar to hemophagocytic lymphohistiocytosis (Cook *et al.*, 2022; Castro *et al*., 2020). Further studies have also shown that patients have alterations in their T cell populations which likely

contributes to the pathogenesis of the disease. Two studies found patients have increased effector memory T cell subsets with decreased populations of naïve T cells with characteristics suggesting a T cell exhaustion phenotype based on RNAseq results (Castro, 2020; Salzer 2021). Studies on patient-derived T cells displayed reduced f-actin density and failure to assemble the actin ring at the synapse (Dupre *et al*., 2021). In addition, studies of patient T cells suggested disruption of the cortical actin network leading to increased release of vesicles and granules (Cook, et al., 2020) . The poor prognosis for patients with this disease as well as the lack of understanding of the role T cell populations play in the disease manifestations warrants further investigation.

In this study, we utilized constitutive and T cell–specific *Nckap1l*-KO mice models to investigate the importance of Hem1 in T cell development and functions. These unique mouse models allow us to study T cell development within the thymus which is unable to be performed in human patients. In addition, we can look at the specific role of Hem1 in T cells and further investigate how abnormalities in this subset of cells contributes to the overall clinical picture including both immunodeficiency and hyperinflammation. Constitutive loss of Hem1 affects all cells of hematopoietic lineage which has been investigated by our group previously in mouse with a loss of function point mutation in *Hem1* (*Hem1*$^{pt/pt}$) (Park, 2008) where we showed defects in erythrocytes, lymphocytes, and granulocytes. We have also generated a conditional *Hem1* knockout mouse utilizing the CreLoxP system and have investigated Hem1's role in specific lineages of hematopoietic cells previously (Suwankitwat *et al*., 2021; Avalos *et al.,* 2022).

This study aims to focus on the role of T cell specific loss of Hem1 on the development, function, and activation of T cells and how this may be harnessed to develop therapies to treat the clinical picture in patients. We hypothesize that disruption of Hem 1 will affect T cell development as well as impair T cell function leading to immunodeficiency and abnormal effector function due to downstream disruptions in f-actin polymerization.

MATERIALS AND METHODS

Animal Models

Nckap1l (Hem1) floxed mice (*Hem1$^{fl/fl}$)* (Suwankitwat, 2021) were bred to mice expressing Cre recombinase under the control of proximal promoter of the lymphocyte protein tyrosine kinase (*pLckCre)* (B6.Cg-Tg(Lck-cre)548Jxm/J) (Hennet, 1995) to generate mice with T cell-specific deletion of Hem-1 early in thymocyte development at the double negative (DN) 2 stage. *Hem1$^{fl/fl}$* mice were also bred to mice expressing Cre recombinase under the under control of the *CD4* enhancer/promoter/silencer sequence (*CD4Cre*) (B6.Cg-Tg(Cd4-cre)1Cwi/BfluJ) (Lee, 2001) to generate mice with T cell-specific deletion of Hem-1 later in thymocyte development at the double positive stage. Mice with constitutive deletion of Hem-1 (*Hem1$^{-/-}$)* were generated as previously described (Suwankitwat, 2021).

Hem1$^{fl/fl}$pLckcre and *Hem1$^{fl/fl}$CD4Cre* mice were screened and maintained by genomic PCR analysis as described for *pLckCre* (XX) and *CD4Cre* (XX) and following amplification with *Hem1$^{fl/fl}$* forward and reverse oligonucleotides (Suwankitwat, 2021). Constitutive *Hem1$^{-/-}$* mice were generated as previously described (Suwankitwat, 2021). Mice were housed under specific pathogen–free conditions. Experiments were performed on mice from generation 3-10 on a C57BL/6J background. No phenotypic differences were noted between male and female mice; thus, both sexes were used in the experiments. Most studies were performed on mice ages 8–20 weeks, with the exception of the autoantibody array and exhaustion phenotyping studies, which were performed between the ages of 38-52 weeks. Littermate controls were utilized whenever possible and in most experiments. Experimental controls, denoted WT, included both *Hem1$^{+/-}$* and *Hem1$^{fl/fl}$* mice when studying the constitutive and conditional knockout models respectively.

Flow Cytometry

Murine thymocytes, splenocytes, and LN cells were harvested and splenocytes underwent an RBC lysis step using ammonium chloride potassium (ACK) lysis buffer (Invitrogen/Life Technologies) prior to staining. Cells were stained with fluorescent dye-conjugated antibodies, including the following: CD3 (145-2C11), CD4 (GK1.5), CD8a (53-6.7, Biolegend), CD25 (7D4, Tonbo Biosciences), CD44, CD62L (MEL-14, Tonbo Biosciences), CD69 (), CXCR5 (L138D7, BioLegend), B220 (RA3-6B2), NK1.1, PD1 (29F.1A12, BioLegend), IL-2 (JES6-5H4,

Biolegend), IL-4, IL-17A (TC11-18H10.1, Biolegend), TNF-a (MP6-XT22, Biolegend), IFN-g (XMG1.2, Biolegend), . Cells were stained with fluorescent dyes: Vybrant™ CFDA SE Cell Tracer Kit (Invitrogen), LIVE/DEAD™ Fixable Near-IR Dead Cell Stain Kit (Invitrogen), and Caspase 3/7 (C10427, Invitrogen).

Intracellular staining was performed using the Fixation/Permeabilization kit (BD Biosciences), and intranuclear staining was performed using the Foxp3 / Transcription Factor Staining Buffer Set (eBioscience). Phosphoprotein staining was performed by fixing cells with paraformaldehyde and permeabilizing with 100% ice cold methanol.

T cell activation

Splenocytes were RBC lysed as described above. Pan T cells were enriched using the Pan T Cell Isolation Kit II (Miltenyi Biotec) by negative selection. Purified T cells (2 x 10^5) were plated in each well of a 96-well plate and stimulated with 10 ug/ml of Ultra-LEAF purified anti-CD3 (17A2, Biolegend) and anti-CD28 antibodies (37.51, Biolegend) for 24 hours. Cells were stained with fluorescent conjugated anti-CD25 (PC61.5, Tonbo Biosciences), anti-CD69 (H1.2F3, BioLegend), and anti-CD4 (GK1.5) and anti-CD8 (53-6.7, Biolegend).

Cell proliferation assay

Splenocytes were enriched for T cells and plated as described above. Purified T cells were stimulated with 10 ug/ml of anti-CD3 and anti-CD28 antibodies as well as 2 ug/ml of soluble anti-CD28 antibody in complete RPMI media (RPMI + L-glutamine, 10% FBS, 1% penicillin streptomycin, 1% MEM amino acids, 1% sodium pyruvate, 0.1% 2-mercaptoethanol) for 72 hours. Cells were stained with 5uM of CFDA Vybrant™ CFDA SE Cell Tracer Kit and fluorescent conjugated anti-CD4 (GK1.5) and anti-CD8 (53-6.7, Biolegend).

Cytokine assays

Splenocytes were enriched for T cells by negative selection (Pan T Cell Isolation Kit II, Miltenyi Biotec) or CD4+ T cells by positive selection (CD4 (L3T4) MicroBeads, Miltenyi Biotec), and equal numbers of cells were stimulated with 10-25 ug/ml of anti-CD3 (17A2, Biolegend) and anti-CD28 (37.51, Biolegend) antibody-coated plates for 72 hours. Supernatant

was collected and analyzed for cytokine and chemokine levels using the Mouse Cytokine Array/Chemokine Array 31-Plex and the Mouse Cytokine Th17 12-Plex Discovery Assay® Array (Eve Technologies, Calgary, AB). IL-2, TNF-a, and IFN-g were re-analyzed at a 1:50 dilution in PBS following oversaturation at full concentration using the Mouse Cytokine Proinflammatory Focused 10-Plex Discovery Assay® Array (Eve Technologies, Calgary, AB).

CD107A assay

Methods modified *Betts et al.* (2003). from Splenocytes were harvested as described above and 10^6 cells were stimulated with 50 ng/ml PMA and 1ug/ml of ionomycin in complete RPMI media for 4 hours. Anti-CD107a antibody was added at the start of stimulation at a 1:100 dilution. Monensin (Biolegend) was added after 1 hour of stimulation. Cells were harvested and stained for appropriate surface markers and analyzed by flow cytometry.

F-actin assays

F-actin assay was described previously (Park, 2008). T cells purified from splenocytes as described above were stimulated as described above for 24 hours. Cells were then stimulated with 50ng PMA (Phorbol 12-myristate 13-acetate, Sigma) and 1ug/ml ionomycin (Sigma) for 15 minutes. Cells were stained for surface markers with fluorescent conjugated antibodies and then fixed, permeabilized, and intracellularly stained with AlexaFluor™ 488 phalloidin (ActinGreen, Invitrogen) per manufacturer guidelines. The intensities of F-actin polymerization were measured by flow cytometry.

For fluorescent confocal microscopy evaluation, T cells were isolated as above and stimulated with 1:1 dilution of Mouse T-Activator Dynabeads for 15 minutes. Cells were stained with phalloidin (see above) and Hoechst 33342 (NucBlue, Invitrogen) and slides prepared via cytospin. Slides were imaged and analyzed by fluorescence microscopy (Nikon Eclipse 50i and Visitech VT-iSIM) after.

Protein array profiling analysis.

Mouse sera were collected, aliquoted, and stored at –80°C. Autoantigen microarrays were manufactured in the Microarray and Immune Phenotyping Core Facility of University of Texas Southwestern Medical Center and analyzed as previously described (Avalos *et al.,* 2022).

Statistics

Data were analyzed using the Student's 2-tailed unpaired t test with equal variance, using GraphPad Prism 9. Normality was assessed using the Shapiro-Wilk normality test, and non-parametric data were analyzed using the Mann-Whitney u test using GraphPad Prism 9. Fisher's exact test was to analyze categorical data using GraphPad Prism 9. $P < 0.05$ was considered significant.

RESULTS

Constitutive disruption of *Hem1* disrupts T cell development and results in hepatosplenomegaly

Humans with LOF mutations in the *NCKAP1L* gene resulting in PID lack Hem1 protein in all hematopoietic tissues. To model this condition in mice, we previously generated Hem1 null (*Hem1*$^{-/-}$) mice using gene targeting technology (Avalos et al., 2022; Suwankitwat et al., 2021). Analyses of T cell development in the thymus of 11–16-week-old *Hem*$^{-/-}$ and littermate control mice by flow cytometry revealed significant reductions in the total number of thymocytes and lymphocytes in peripheral lymph nodes (Figure 1A). This reduction in cellularity was reflected as decreased αβ T cells following constitutive disruption of Hem1 in both tissues (Figure 2A and C). In the thymus, this reduction in T cells resulted in decreased double positive (DP) thymocytes (Figure 2A) which is similar to previous results from the *Hem1*$^{pt/pt}$ constitutive model, where thymocyte development was halted at the double negative (DN) to DP transition (Park, 2008). In addition, the lymph nodes had decreased numbers of both CD4^{+} and CD8^{+} T cells (Figure 2C). Other mouse models of Hem1 deficiency have shown decreased tissue migration of macrophages and B cells *in vivo*, secondary to decreased f-actin polymerization which may imply decreased T cell migration to the periphery (Avalos 2022, Suwankitwat 2021).

In addition to alterations in T cell populations. we have previously shown several other hematopoietic cell disruptions in the face of Hem1 deficiency (Park, 2008; Chan, 2013; Suwankitwat, 2021; Avalos *et al.,* 2022). We have observed clinical manifestations of these abnormalities in the Hem1 null mice, including decreased body weight (Avalos *et al.,* 2022), and hepatosplenomegaly (Figure 1B and C). Hepatosplenomegaly is also a feature shared by children with Hem1 deficiency (Cook *et al.*, 2020; Castro *et al.*, 2020; Salzer *et. al*, 2020).

Increased representation of regulatory T cells in Hem1 null mice

T regulatory (Treg) cells are a subset of CD4^{+} helper T cells that are critical for immune tolerance and homeostasis and are characterized expression of the transcription factor FoxP3 (Hori, 2003; Fontenot, 2003; Khattri, 2003). The representation of regulatory T cells was found to be either normal (Cook et al., 2020), or decreased (Castro *et al.*, 2020) in Hem1 PID patients. We wanted to characterize the effect constitutive deletion of *Hem1* on Treg cells. Treg cells

were identified as CD4+CD25+FoxP3+ cells using flow cytometry, and cells from the thymus, spleen, and peripheral lymph nodes from 11-16-week-old *Hem1*$^{-/-}$ and littermate controls. *Hem*$^{-/-}$ mice had increased frequency of Treg cells in the thymus, spleen, and lymph nodes, however we did not observe any change in absolute numbers of Treg cells (Figure 3A and B). Since the total αβT cells were reduced in *Hem1*$^{-/-}$ mice, this suggests the ratio of immunosuppressive Treg cells to effector T cells is increased which may play a role in the overall reduced immune effector function in Hem1 null mice.

In addition, we looked at T follicular helper (T_{FH}) cells in the Hem1 null mouse. T_{FH} cells are a subset of $CD4^+$ T cells that assist B cell function by supporting high-affinity antibody production and the development of memory B cells (Gensous, 2018). No obvious abnormalities were noted in T_{FH} populations in Hem1 PID patients (Salzer, 2020). We defined the T_{FH} population via flow cytometry by gating on $CD4^+$PD-1+CXCR5+ cells and confirming with intracellular Bcl-6^{hi} expression (Figure 3C). Hem1 null mice have increased frequencies of T_{FH} cells in the spleen, however we did not see a significant increase in the absolute number of T_{FH} cells which is consistent with the findings from Salzer et al. (Figure 3D) (Salzer, 2020). B cells also have markedly decreased antibody production in B cell specific Hem1 deficient mice (Avalos *et al.,* 2022), which suggests that T_{FH} may not play an important role in this process. In addition, unregulated T_{FH} activity has been implicated in leading to autoimmune manifestations (Gensous, 2018), and B cell specific Hem1 deficient mice have been shown to produce higher amounts of autoantibodies and Hem1 PID patients exhibit autoimmune manifestations as well (Avalos *et al.,* 2022; Cook *et al.*, 2022).

Decreased naïve and increased memory T cells in Hem1 null mice

Naïve T cells are essential for recognizing new antigens, and once primed by antigen, can develop into memory or effector T cells. Central memory cells tend to reside in secondary lymphoid tissues, while effector memory cells reside in lymphoid and peripheral tissues waiting to recognize antigen for re-activation (Roberts *et al.*, 2005). Memory T cells mount a faster and more robust immune response on re-activation to recall antigens. One of the key features of altered T cell phenotype in human Hem1 PID patients included an increase in $CD4^+$ and $CD8^+$ memory T cells with a subsequent decrease in naïve T cells in several patients (Cook *et al.*, 2020; Castro *et al.*, 2020; Salzer *et. al*, 2020). We evaluated naïve ($CD44^-CD62L^+$), central

memory ($CD44^+CD62L^+$), and effector memory ($CD44^+CD62L^-$) T cells in the spleen and peripheral lymph nodes harvested from Hem1 null and littermate controls by flow cytometry. Similarly, we saw a decrease in the frequency and total number of naïve T cells in secondary lymphoid tissue in Hem1 null mice compared to littermate controls (Figure 4). In response to decreased naïve T cells, effector memory cell frequencies were increased in the periphery. The peripheral lymph nodes also had total increased numbers of effector memory T cells (Figure 4B). These results suggest that constitutive loss of Hem1 in both humans and mice results in a shift towards increased effector memory T cells.

Reduced frequency of CD8 T cells and increased regulatory and memory T cells in T cell specific Hem1 deficient mice

Since constitutive disruption of Hem1 mimics many aspects of T cell deficiency in Hem1 PID in humans, we next sought to isolate which of these abnormalities are specific to T cell disruption of *Hem1.* For these studies, we utilized the CreLoxP system where we bred Hem1floxed mice (Suwankitwat *et al*., 2021) to mice expressing Cre under control of either the Lck proximal promoter (pLckCre), which deletes floxed flanked alleles early in thymocyte development during the double negative stage (Hennet *et al.,* 1995), or CD4Cre which deletes floxed flanked alleles later during the DP stage of T cell development (Lee et al., 2010). The pLckCre mouse has robust excision in thymocytes, and we first used this model when studying T cell development due to its expression early in thymocyte development. However, pLckCre has a slightly lower excision rate in mature T cells (66-83% in splenic $CD4^+$ T cells) (Hennet *et al*., 1995), so we also studied CD4cre mice which have a high excision rate >99% at the DP stage of thymocyte development. The results from the $Hem1^{fl/fl}CD4cre$ mice were similar to those from the $Hem1^{fl/fl}pLckCre$ mice.

We harvested thymus, spleen, and peripheral lymph nodes (axillary and inguinal, pooled) from $Hem1^{fl/fl}$ *pLckCre* and $Hem1^{fl/fl}$ littermate controls and examined T cell populations via flow cytometry. Similar to the $Hem1^{-/-}$ mice, $Hem1^{fl/fl}$ *pLckCre* mice had decreased frequencies of DP thymocytes, and the subsequent increase in DN cells suggests an issue with the DN to DP transition during thymocyte development (Figure 5A). The spleen and lymph nodes from $Hem1^{fl/fl}$ *pLckCre* mice also had decreased proportions of αβ T cells compared to littermate controls, however there was no change in absolute numbers (Figure 5B and C). In

addition, there was a decreased proportion of $CD4^+$ T and $CD8^+$ T cells in the spleen and lymph nodes respectively (Figure 5B and C).

Interestingly, the representation of $CD4^+FoxP3^+$ Tregs was increased in thymus, spleen, and lymph node, as we had seen in *Hem1*$^{-/-}$ mice (Figure 6A, B). The percentage and total number of T_{FH} cells were not different between *Hem1*$^{fl/fl}$*pLckCre* mice versus littermate control mice (Figure 5C), suggesting that the increased representation of T_{FH} cells we see in *Hem1*$^{-/-}$ mice may be reflective of reductions of other hematopoietic lineage cells.

We next assessed the representation of naïve and memory T cells following T cell specific disruption of Hem1. As we had previously seen in *Hem1*$^{-/-}$ mice, we found decreased representation of naive CD4 and CD8 T cells and increased representation of effector memory CD4 and central memory CD8 T cells in spleens from *Hem1*$^{fl/fl}$*pLckCre* mice versus littermate control mice (Figure 7). These results suggest that Hem1 has a central role in regulating T cell memory in a T cell specific manner.

Decreased activation and division of CD4 T cells and increased inhibitory receptor expression in T cell specific Hem1 deficient mice.

T cell immune synapses are highly dependent on Arp2/3-mediated f-actin polymerization (Dupre *et al*., 2019). Due to disruptions in f-actin with Hem1 deficiency, Hem1 deficient T cells fail to properly process antigen signals and fully activate. This was evident with T cells from Hem1 PID patients that exhibit reduced activation and proliferation profiles regardless of naïve and memory status (Cook *et al.*, 2020; Castro *et al.*, 2020; Salzer *et. al*, 2020). This was also previously shown by Park et al. in mice with a constitutive loss of Hem1 secondary to a point mutation in *Hem1* with decreased CD69 expression and decreased proliferation (Park *et al*., 2008).

To examine how T cell specific disruption of Hem1 effected T cell activation, we measured the upregulation of the early activation markers CD69 and CD25 following 24 hrs of anti-CD3 and anti-CD28 stimulation. We found that there was a significant reduction in both CD69 and CD25 upregulation in CD4 T cells but not CD8 T cells in *Hem1*$^{fl/fl}$*pLckCre* mice versus littermate control mice (Figures 9A and B). In addition, mean forward light scatter (FSC), a measure of cell size, was significantly lower in *Hem1*$^{fl/fl}$*pLckCre* mice versus littermate control mice consistent with reduced T cell activation (Figure 9C). Next, we labeled cells with CFSE to

measure proliferation following 72 hrs of anti-CD3/anti-CD28 stimulation, and we found a significant reduction in proliferation in $CD4^+$ T cells but no difference in $CD8^+$ T cells (Figure 9D).

Decreased T cell response to stimulation may be secondary to increased apoptosis or T cell exhaustion. Splenocytes and lymphocytes were harvested from *Hem1$^{fl/fl}$CD4Cre* mice and *Hem1$^{fl/fl}$* littermate control mice, and we evaluated $Caspase3^+$ apoptotic cells and dead cells (Live/Dead-Near IR) by flow cytometry. No difference was seen in the frequency of T cells undergoing apoptosis, however there was increased representation of dead $CD4^+$ and $CD8^+$ T cells in the lymph nodes in *Hem1$^{fl/fl}$CD4Cre* mice compared to controls (Figure 9C). Decreased activation in $CD4^+$ T appears to be unrelated to increased induction of apoptosis.

T cells from Hem1 deficient patients were also characterized as having "exhausted" phenotype, exemplified by increased memory T cells, reduced T cell proliferation, reduced upregulation of activation markers such as CD69 and CD25, and increased inhibitory receptor expression (Castro *et al.*, 2020; Salzer *et al.*, 2020). Due to the similarities in activation and proliferation, we sought to evaluate an "exhausted" T cell phenotype in aged Hem1 deficient mice by looking at the co-expression of inhibitory molecules PD-1 and Tim-3 on T cells from the spleen and lymph nodes. We found that T cell specific disruption of Hem1 resulted in significantly increased expression of $CD4^+$ $^aCD44^+Tim3^+PD1^+$ and $CD8^+CD44^+Tim3^+PD1^+$ cells, consistent with increased T cells with an "exhausted" phenotype.

Increased cytokine production, reduced cortical actin, and increased granule membrane fusion following T cell specific disruption of Hem1.

Since Hem1 disruption led to altered T cell activation and homeostasis, especially in $CD4^+$ T cells, we sought to investigate if there was subsequent altered cytokine production. Our preliminary experiment involved purifying pan T cells from splenocytes from *Hem1$^{fl/fl}$pLckCre* and littermate controls. T cells were stimulated *in vitro* with anti-CD3/anti-CD28 for 72 hrs and supernatant was analyzed for cytokine levels via multiplex bead cytokine array. We found Hem1 deficiency resulted in decreased IL-2 and markedly increased IL-10 and IL-17 production (Figure 10A).

To further elucidate the contribution from CD4 T cells, we repeated this experiment with purified $CD4^+$ T cells isolated from splenocytes harvested from *Hem1$^{fl/fl}$CD4Cre* mice. We

found Hem1 deficient $CD4^+$ T cells produced significantly more IFNγ (Figure 10B). In addition, we found Hem1 deficient $C4^+$ T cells also produced more of the Th2 cytokines IL-5 and IL-13 compared to control T cells (Figure 10B). As we had seen with stimulation of total T cells, Hem1 deficient CD4 T cells produced significantly more of the Th17 cytokines IL-17 and IL22, and increased IL-10 (Fig 10B). These results suggest that Hem1 deficient CD4 T cells have a hypersecretory cytokine phenotype.

To evaluate cytokine production, we also evaluated intracellular levels of cytokines on an individual cell basis using flow cytometry. We purified T cells from splenocytes from *Hem1$^{fl/fl}$CD4Cre* mice and littermate controls and stimulated them with anti-CD3/anti-CD28 for 72 hrs followed by stimulation with PMA/ionomycin for 5 hours. Cells were permeabilized followed by intracellular labeling. Similarly, Hem1 disruption decreased the proportion of $CD4^+$ T cells producing IL-2 with lower MFI (or intensity), while the proportion or intensity was increased for TNFα, IFNγ, and IL-17 (Figure 10C). In addition, there was increased frequency of Hem1 deficient $CD8^+$ T cells producing TNFα and IFNγ (Figure 10C).

Increased production of cytokines as well as increased release of cytokines may contribute to the increased levels of cytokines seen in our previous assays. F-actin forms a cortical actin barrier around the periphery of the cells which plays a key role in regulating vesicle and granule release (Cook *et al.*, 2022). Disruption of the cortical actin secondary to Hem1 deficiency has been previously shown in Hem1 PID humans (Cook *et al.*, 2020). We sought to measure total f-actin expression following stimulation in T cells to see if this would correlate with decreased cortical f-actin. Splenocytes were harvested from *Hem1$^{fl/fl}$pLckCre* mice and littermate controls and stimulated with anti-CD3/anti-CD28 for 24 hrs followed by PMA/ionomycin stimulation for 15 minutes. Cells were stained with phalloidin and measured via flow cytometry. Our results did not show any significant decrease in actin expression in Hem1 deficient T cells compared to control T cells, however there was a slight shift in MFI between the groups (Figure 11A).

Several studies in human patients also found Hem1 disruption led to increased expression of surface CD107A (LAMP-1) (Cook *et al.*, 2020; Castro *et al.*, 2020). CD107A is expressed on vesicles intracellularly, however, is expressed on the surface of the cell following fusion of the vesicle with the cell membrane during exocytosis. We harvested splenocytes from

Hem1$^{fl/fl}$*CD4Cre* mice and littermate controls and stimulated the cells with PMA/ionomycin while co-incubating with fluorescently tagged anti-CD107A antibody and monensin for 5 hrs. We found significant upregulation of surface CD107A in $CD4^+$ and $CD8^+$ T cells with increased MFI in the Hem1 deficient cells compared to controls (Figure 11C). These findings suggest that Hem1 disruption leads to dysregulation of the cortical actin barrier and increased release of cytokines from $CD4^+$ T cells and may provide a possible mechanism for our data.

Hem1 disruption results in impaired T cell immune synapse formation and f-actin rearrangement.

When T cells recognize antigen via the TCR, the cells form a prolonged contact with the antigen presenting cell known as the immune synapse, and actin is a critical component for immune synapse assembly and sustained signal transduction (Calvez *et al*., 2011). Dysregulation of f-actin polymerization secondary to actinopathies, including Hem1 PID, has been shown to decrease synapse formation and downstream immune cell signaling and activation (Dupre *et al*., 2021; Cook *et al.*, 2020; Calvez *et al*., 2009). We sought to examine the immunological synapse formation and adhesion in Hem1 deficient T cells. T cells were purified from *Hem1*$^{fl/fl}$*pLckCre* mice and littermate controls, stimulated with anti-CD3/anti-CD28 coated beads to mimic an antigen presenting cell for 15 minutes. Cells were fixed and permeabilized and stained for actin with phalloidin and Heoscht 33342. Cytopsin slides were prepared and TCR-induced capping formation and adhesion was observed using fluorescent microscopy. Hem1 deficient T cells had a lower frequency of TCR-induced actin capping at the immunological synapse compared to littermate control T cells, and in addition there was a significant relationship between actin capping and Hem1 status (Figure 11B). These results are in line with data from human Hem1 deficient T cells as well as previous studies in constitutively deficient Hem1 mouse models (Cook *et al.*, 2020; Park *et al*., 2008). Inadequate immune synapse formation likely leads to decreased signaling following TCR binding and decreased activation and effector function.

T cell specific disruption of Hem1 does not result in increased autoantibody formation

Increased autoantibody production is one feature of humans with LOF mutations in Hem1(Salzer *et al.*, 2020), and increased autoantibodies were noted in constitutive Hem1 null

mice (Salzer *et al.*, 2020) and B cell specific Hem1 deficient mice (Avalos *et al.*, 2022). Given the alterations in T cell signaling and cytokine release in our murine models, we next assessed whether T cell specific disruption of Hem1 was sufficient to result in increased autoantibody production. Sera were collected from aged female *Hem1*$^{fl/fl}$*pLckCre* mice and littermate controls (49-56-weeks-old), and autoantibody production was assessed using autoantigen microarray technology containing 128 autoantigens. No increases in autoantibodies were noted (Figure 12), suggesting that loss of Hem1 in T cells may not be the primary driver of increased autoantibodies in humans.

DISCUSSION

The severe primary immunodeficiency disorders (PID) and autoimmune disease manifestations seen in patients with loss-of-function mutations in the gene encoding Hem1 warrant further investigation into the cell-specific role Hem1 plays in immune homeostasis. Unfortunately, PIDs in humans are usually diagnosed at an advanced stage of disease progression with delayed diagnosis and misdiagnosis common (Shearer *et al*., 2007; Wu *et al*., 2019). Studying the underlying mechanisms of disease pathogenesis may be complicated by infection, hyperinflammation, autoimmunity, and immunosuppressive treatments. Our study utilized mice with constitutive and T cell specific deletion of *Hem1* to further characterize the role Hem1 plays in T cell development and function, in addition to how T cells specifically contribute to the overall clinical picture seen in patients. Our results suggest that Hem1 plays a role in regulating development, homeostasis, and effector functions of $CD4^+$ T cells. In addition, we've shown remarkable similarities between the mouse models studied and what was found in human patients afflicted with loss of function mutations in *Hem1*, suggesting that our mouse models can provide a critical tool to further understand the disease process in humans and hopefully provide an avenue for studying potential therapeutics.

The constitutive mouse model recapitulated hepatosplenomegaly as seen in most patients with Hem1 deficiency, and we saw an approximately 6-fold and 4-fold reduction in cellularity in the thymus and lymph nodes respectively, which was likely secondary to lymphopenia as previously shown (Park *et al*., 2008; Suwankitwat *et al*., 2021).

Both mouse models (constitutive and conditional T cell deletion of *Hem1*) resulted in a decrease in the absolute number or proportion of αβ T cells in the periphery (spleen and LN), which correlated with a subsequent increase in the proportion of γδ T cells (data not shown). There was also a reduction in the proportion of $CD4^+$ T cells with a shift in the CD4:CD8 ratio, suggesting the $CD4^+$ T cells are more affected by the loss of Hem1. Similar findings were shown in human patients as well, coupled with selectively reduced effector function in $CD4^+$ T cells (Cook *et al.*, 2020; Castro *et al.*, 2020). Interestingly, we also found an increased representation of Treg cells in both the constitutive and conditional models, coupled with an approximately 7-fold increase in IL-10 cytokine production by $CD4^+$ T cells in the conditional mouse model. Increased serum IL-10 was identified in Hem1 deficient patients (Castro *et al*., 2020), however

no change (Cook *et al.*, 2020) or decreased Treg cells (Castro *et al*., 2020) were seen in human patients with Hem1 PID. Coupled with our findings of increased IL-17, increased IL-10 may also be produced by immunosuppressive Th17 cells which co-express IL-10 and IL-17, since no changes in Treg numbers were observed. These results suggest an increase in T cell immunosuppressive function in our mouse models of Hem1 which may impair T cell homeostasis and immune function in Hem1 deficient mice and humans.

In addition to a reduction in the representation of CD4 T cells, constitutive disruption of Hem1 resulted in a reduction of naïve CD4 and CD8 T cells and increased effector memory CD4 and CD8 splenic T cells. Similarly, T cell specific disruption of Hem1 resulted in decreased naïve CD4 and CD8 splenic T cells and increased effector memory CD4 T cells. Decreased naïve T cells and increased central and effector memory cells was a hallmark of Hem1 PID in humans, and one of the most consistent findings between patients regarding T cell abnormalities (Cook *et al.*, 2020; Castro *et al.*, 2020; Salzer *et. al*, 2020). These findings suggest that there may be increased effector memory T cells in the face of chronic, recurrent infections and/or secondary to a hyperinflammatory or autoimmunity state in patients. We also found increased expression of the T cell exhaustion markers PD-1 and Tim-3 by Hem1 deficient T cells, suggesting chronic stimulation may lead T cells to exhibit an exhausted phenotype.

Actin plays a role in TCR activation and immune synapse formation and TCR signaling, so we sought to assess the effect of Hem1 on T cell activation and proliferation. Human Hem1 PID resulted in decreased activation and proliferation (Cook *et al.*, 2020; Castro *et al.*, 2020; Salzer *et. al*, 2020), and T cells from Hem1 deficient patients had decreased upregulation of CD25 and CD69 following stimulation (Cook *et al.*, 2020; Castro *et al.*, 2020; Salzer *et. al*, 2020). In addition, perturbations in T cell proliferation were seen in several patients with blunted proliferation in either $CD4^+$ T cells only (Cook *et al.*, 2020) or both CD4 and CD8 T cells (Salzer *et al*., 2020). We found Hem1 deficient CD4+ T cells had decreased expression of CD69 and decreased proliferation, while $CD8^+$ T cells were unaffected. We observed similar trends with CD25 expression. Hem1 deficient CD4 T cells were decreased in size also suggesting decreased activation.

Decreased activation may be caused by weak TCR signaling secondary to improper immune synapse formation from disrupted f-actin polymerization. We assessed immune synapse formation and adhesion by fluorescent microscopy and found decreased actin-capping at the

junction between T cells and anti-3/anti-CD28 coated beads which mimic the immune synapse with an antigen presenting cell. Decreased activation in Hem1 deficient T cells may also be related to the increased exhausted phenotype we observed since exhausted T cells have difficulty mounting a proper immune response and express inhibitory receptors (Wherry *et al*., 2015).

Additionally, Hem1 deficient B and T cells in human patients had selective decreased signaling through the mechanistic target of rapamycin-containing complex 2 (mTORC2) pathway resulting in decreased phosphorylation of AKT at serine 473 (a specific target of the mTORC2 pathway) (Cook *et al.*, 2020; Salzer *et al*, 2020). Decreased AKT activation was similarly observed in a constitutive model of Hem1 null mice and was thought to drive decreased B cell proliferation and survival (Salzer *et al*., 2020). Actin has also previously been shown to be linked to mTORC2 in a negative feedback loop where increased plasma membrane tension activates mTORC2 which in turn downregulates actin nucleation (Diz-Munoz *et al*., 2016). Interestingly, a model of T cell specific Wave2 deficiency has shown the opposite with upregulation of mTORC1 and mTORC2 resulting in hyperinflammation and autoimmunity (Liu *et al*., 2021). Further investigation into the mTOR signaling pathway is warranted in our mouse model to see if mTOR signaling alterations contribute to the activation and proliferation abnormalities we observed.

Actin also forms a dense ring of cortical actin at the cell perimeter which is thought to serve as a barrier to unregulated vesicle exocytosis and release of cell mediators such as granzymes and cytokines (Cook *et al.*, 2022). We looked at cytokine production in Hem1 deficient T cells and found decreased production of IL-2 which, similar to findings from Cook *et al.* in Hem1 deficient humans (Cook *et al.*, 2020). Concurrently, Hem1 deficient $CD4^+$ T cells also had decreased intracellular IL-2 which suggests decreased production of IL-2. We also found that Hem1 deficient T cells released significantly increased amounts of the Th1 cytokine IFNγ, Th2 cytokines IL-5, IL-13, Th17 cytokines IL-17, IL-22, and the Treg cytokine IL-10 from purified CD4 T cells following anti-CD3/anti-CD28 stimulation. We also saw increased production of IFNγ, IL-10, and IL-17 via intracellular cytokine staining. We had previously shown that T cells from mice with a constitutive disruption of Hem1 secondary to a loss of function point mutation produced increased levels of IL-17 in serum and following in vitro stimulation (Park *et al.*, 2008). Human Hem1 PID patients were also found to have elevated IFNγ and IL-10 (Castro *et al*., 2020; Salzer, *et al*. 2020). Since so many different cytokines were

altered, we investigated ways to measure dysfunction of the cortical actin barrier which may result in nonspecific hypersecretion of cytokines. We saw increased surface expression of CD107A in CD4 and CD8 T cells secondary to stimulation, suggesting increased exocytosis of granules and cytokines secondary to dysfunction of the cortical actin barrier. These findings mimic the findings in human studies (Cook *et al.*, 2020; Castro *et al.*, 2020). The changes in the levels and types of cytokines released by Hem1 deficient CD4 T cells is likely multifactorial, a combination of altered production and release secondary to disruptions in f-actin polymerization.

The consistent elevation in IL-17 production by Hem1 deficient T cells in our past studies in the constitutive *Hem1*$^{pt/pt}$ mouse and our current studies in T cell specific Hem1 null mice further supports that IL-17 may play a major role in the disease progression. We also found increased levels of IL-22, another cytokine produced by Th17 cells. Autoimmunity and hyperinflammation are common features of disease in Hem1 deficient patients, with the production of autoantibodies, immune mediated thrombocytopenia following vaccination, and atopic disease affecting patients (Cook *et al.*, 2020; Castro *et al.*, 2020; Salzer *et. al*, 2020; Cook *et al.,* 2022).

IL-17 is a proinflammatory cytokine that provides protection from extracellular pathogens normally, however it also plays a role in autoimmune disease (Gensous *et al*., 2020; Kuwabara *et al*., 2017). Excessive Th17 cells that produce excessive IL-17 and GM-CSF and have been implicating in driving autoimmune disease, such as multiple sclerosis and rheumatoid arthritis (Kuwabara *et al*., 2017; Mills *et al*., 2022). IL-17 has also been implicated in inflammatory bowel disease (IBD) and has been shown to be increased in the gastrointestinal mucosa and serum of patients with IBD (Fujino *et al*., 2003). In addition, GWAS studies also suggest that *Hem1* is a key driver gene in inflammatory bowel disease (Peters *et al*., 2017), and increased frequencies of IL-17A positive cells were found in intestinal lamina propria of *Hem1*$^{pt/pt}$ mice deficient in Hem1.

IL-17 has also been proposed to play a major role in Th2 low asthma and atopy. IL-17 is thought to be involved in the neutrophilic inflammation and airway remodeling processes in severe asthma (Chesne *et al*., 2014). Several studies also showed that concurrent increased expression of IL-17 and IL-22 in mononuclear cells and bronchial biopsies correlated with more severe asthma that was resistant to steroids (Badi *et al*., 2022; Ricciardolo *et al.,* 2017; Wang *et al.*, 2017; Zhu *et al*., 2011). In addition, increased serum IL-17 was consistently noted in

patients with food allergies, allergic rhinitis, and atopic dermatitis, and higher IL-17 correlated with the severity of disease (Hofmann *et al.*, 2021).

Increased IL-17 secondary to Hem1 disruption in patients likely contributes to the disease progression towards atopy and autoimmune disease, which may provide a possible avenue for treatment for patients. Anti-IL-17 monoclonal antibody therapies are already used in treating patients with immune mediated inflammatory disease including psoriasis and rheumatoid arthritis (Mills *et al.,* 2022), and promising results have been shown with IL-17 inhibitors in murine models of asthma in preclinical studies (Liang *et al.,* 2018; Carmago *et al*., 2020; Carmago *et al*., 2018). Blockade of IL-17 using anti-IL-17 antibodies murine models of asthma contributed to the control of airway inflammation, extracellular matrix remodeling, oxidative stress, and decreased goblet cell numbers and mucus secretion (Liang *et al*., 2018; Carmago *et al*., 2018).

We have shown that the constitutive and T cell specific murine models of Hem1 deficiency share many hallmarks of the disease observed in human patients with Hem1 PID. In addition, these models allow us to further investigate the role of T cells in the disease and help delineate the roles immune cells play in the disease progression. Our studies revealed that disruption of Hem1 in T cells results in in T cells being skewed towards memory cells with increased expression of T cell exhaustion markers, lymphopenia with decreased $CD4^+$ T cells, decreased $CD4^+$ T cell activation and proliferation, as well as increased cytokine release and production likely secondary to defects in f-actin polymerization. Our studies found Hem1 plays an important role in T cell activation and homeostasis, and the mouse models we employed provide an opportunity to further study the disease of Hem1 PID and potential therapeutic avenues for the patients affected by this disease.

FIGURES

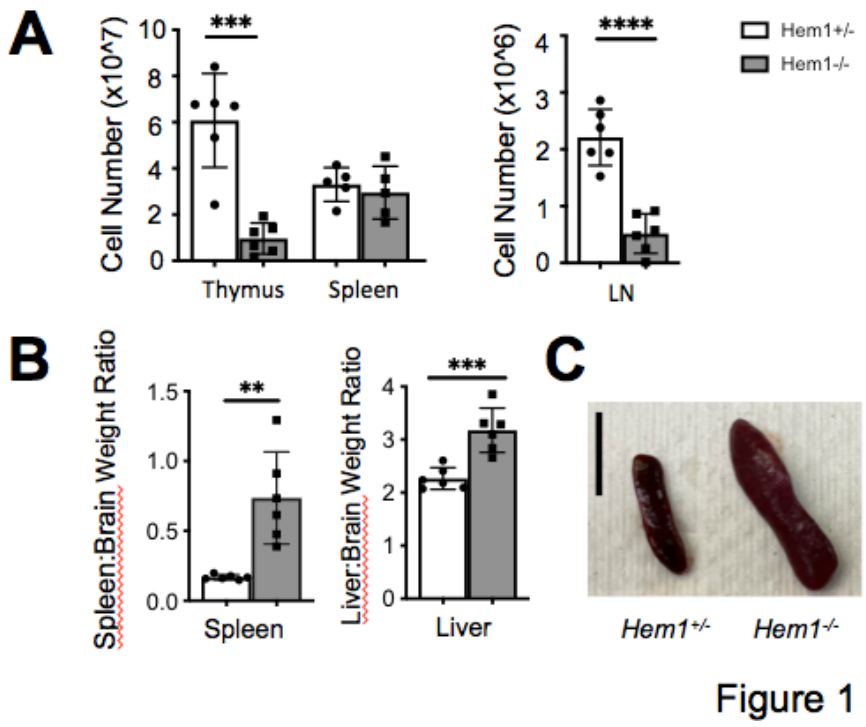

Figure 1. Constitutive disruption of *Hem1* results in decreased cellularity in the thymus and peripheral lymph nodes, as well as hepatosplenomegaly.

(A) Total thymocytes, splenocytes, and cells from axial and inguinal lymph nodes were isolated from *Hem1*$^{-/-}$ mice and *Hem1*$^{+/-}$ littermate controls. Cell counts were calculated using Countbright absolute counting beads by flow cytometry. Bar graphs represent the total cellularity in each organ specified. **(B)** Spleen, liver, and brains were harvested from *Hem1*$^{-/-}$ mice and *Hem1*$^{+/-}$ littermate controls. Spleen and liver were weighed and normalized to brain weights from the same individual mouse (Sellers *et al.*, 2007). Bar graphs represent the ratio of spleen: brain and liver: brain weights. **(C)** Representative image of spleens harvested from *Hem1*$^{+/-}$ control (left) and *Hem1*$^{-/-}$ (right) mice. Line represents 1cm. 11–16-week-old mice, n=6/group, each data point represents an individual mouse. Data are representative of 2 or more independent experiments. Bar graphs represent mean ± SD and were analyzed via unpaired Student's t test. $^{**}P < 0.01$, $^{***}P < 0.001$, $^{****}P < 0.0001$.

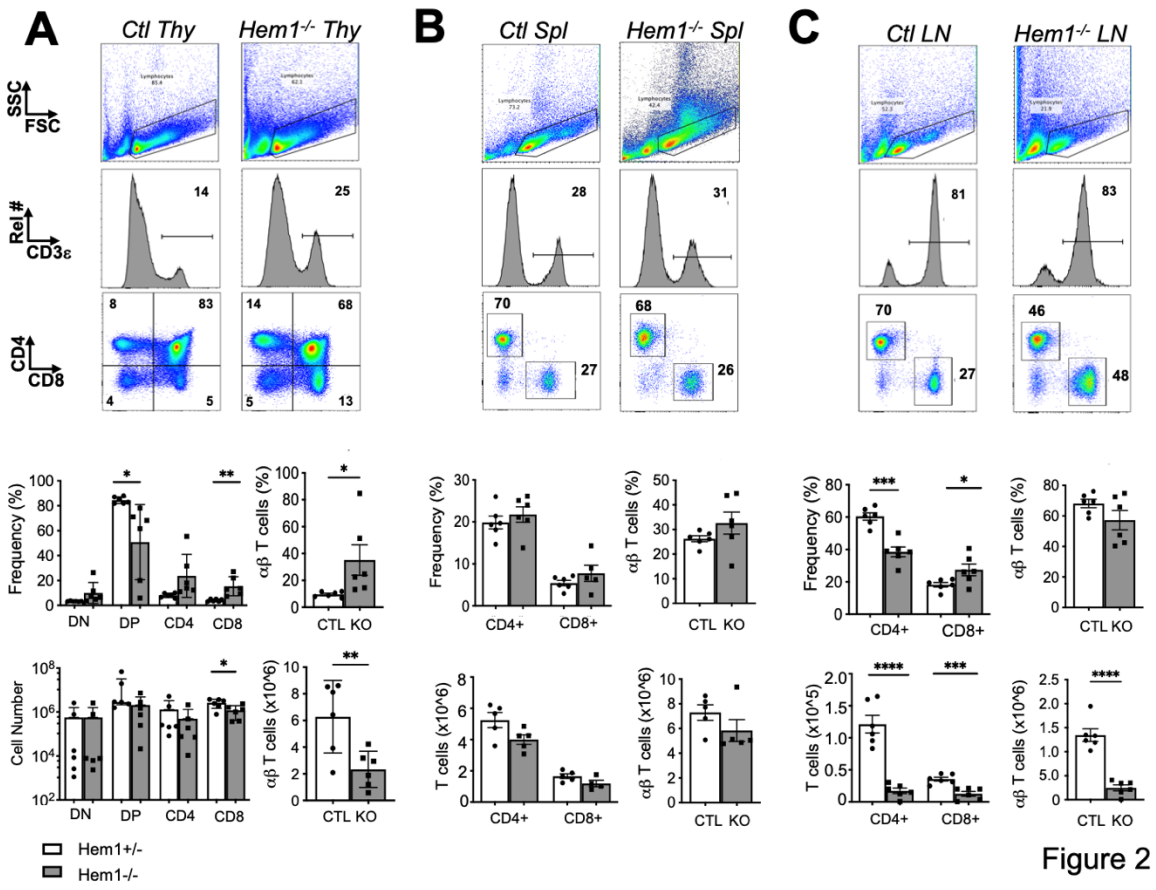

Figure 2. Constitutive disruption of *Hem1* disrupts T cell development

Total thymocytes, splenocytes, and cells from axial and inguinal lymph nodes were isolated from *Hem1*$^{-/-}$ mice and *Hem1*$^{+/-}$ littermate controls. T cell populations were analyzed by flow cytometry. **(A)** Representative flow cytometric dot plot histograms of thymocytes (top). Bar graphs and quantification of double negative (DN), double positive (DP), $CD4^{+}CD8^{-}$ (CD4), and $CD8^{+}CD4^{-}$ (CD8) cells in the thymus (bottom). **(B)** Representative flow cytometric dot plot histograms of splenocytes (top). Bar graphs and quantification of $CD4^{+}$ and $CD8^{+}$ T cells (bottom). **(C)** Representative flow cytometric dot plot histograms of cells from the axillary and inguinal lymph nodes combined (top). Bar graphs and quantification of $CD4^{+}$ and $CD8^{+}$ T cells (bottom). 11–16-week-old mice, n=6/group, each data point represents an individual mouse. Data are representative of 2 or more independent experiments. Bar graphs represent mean ± SD and were analyzed via unpaired Student's t test. **P* < 0.05, ***P* < 0.01, ****P* < 0.001, *****P* < *0.0001*.

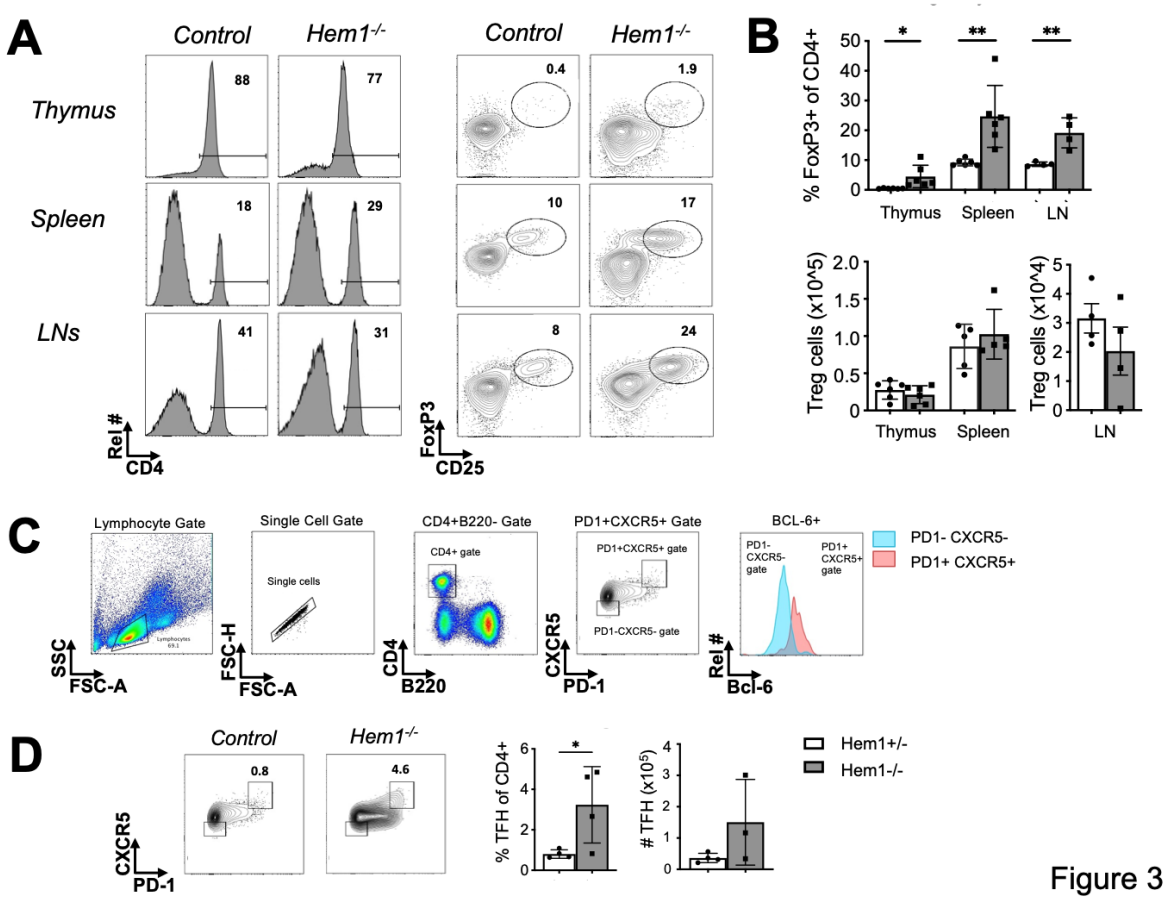

Figure 3

Figure 3. Constitutive disruption of *Hem1* results in increased proportion of regulatory T cells and T follicular helper cells.

(A and B) Total thymocytes, splenocytes, and cells from axial and inguinal lymph nodes were isolated from 11-16-week-old (n=6/group) *Hem1*$^{-/-}$ mice and *Hem1*$^{+/-}$ littermate controls. Representative flow cytometric dot plot histograms **(A)**, and bar graphs and quantification of T regulatory cells ($CD4^+CD25^+FoxP3^+$) **(B)**. 11–16-week-old mice, n=6/group, data representative of 2 independent experiments. **(C and D)** Total splenocytes were isolated from 11-12-week-old (n=3-4/group) *Hem1*$^{-/-}$ mice and *Hem1*$^{+/-}$ littermate controls. Representative flow cytometric dot plot histograms with gating strategy for T follicular helper cells ($CD4^+CXCR5^+PD\text{-}1^+$). Bar graphs and quantification of T follicular helper cells (D). Each dot represents an individual mouse. Bar graphs represent mean ± SD and were analyzed via unpaired Student's t test. **P* < 0.05, ***P* < 0.01, ****P* < 0.001. Treg = regulatory T; TFH = T follicular helper

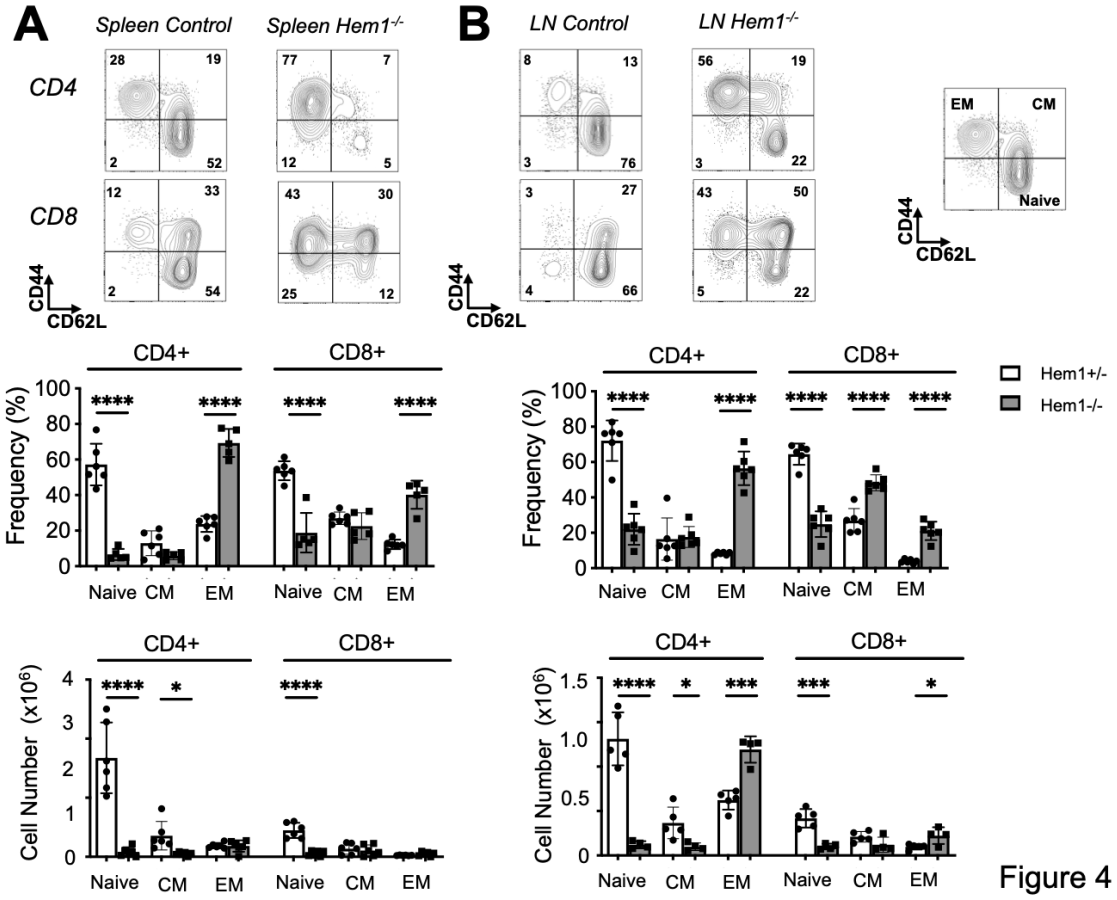

Figure 4. Constitutive disruption of *Hem1* results in decreased naïve T cells with a concurrent increase in effector memory T cells.

Total splenocytes and cells from axial and inguinal lymph nodes were isolated from *Hem1*$^{-/-}$ mice and *Hem1*$^{+/-}$ littermate controls. **(A)** Representative flow cytometric dot plot histograms of splenocytes (top). Bar graphs and quantification of naïve (CD44^{-}CD62L^{+}), central memory (CD44^{+}CD62L^{+}), and effector memory (CD44^{+}CD62L^{-}) T cells from splenocytes (bottom). **(B)** Representative flow cytometric dot plot histograms (top) and bar graphs (bottom) of T cells harvested from lymph nodes. 11–16-week-old mice, n=6/group, each data point represents an individual mouse. Data are representative of 2 independent experiments. Bar graphs represent mean ± SD and were analyzed via unpaired Student's t test. **P* < 0.05, ****P* < 0.001, *****P* < 0.0001. CM = central memory; EM = effector memory.

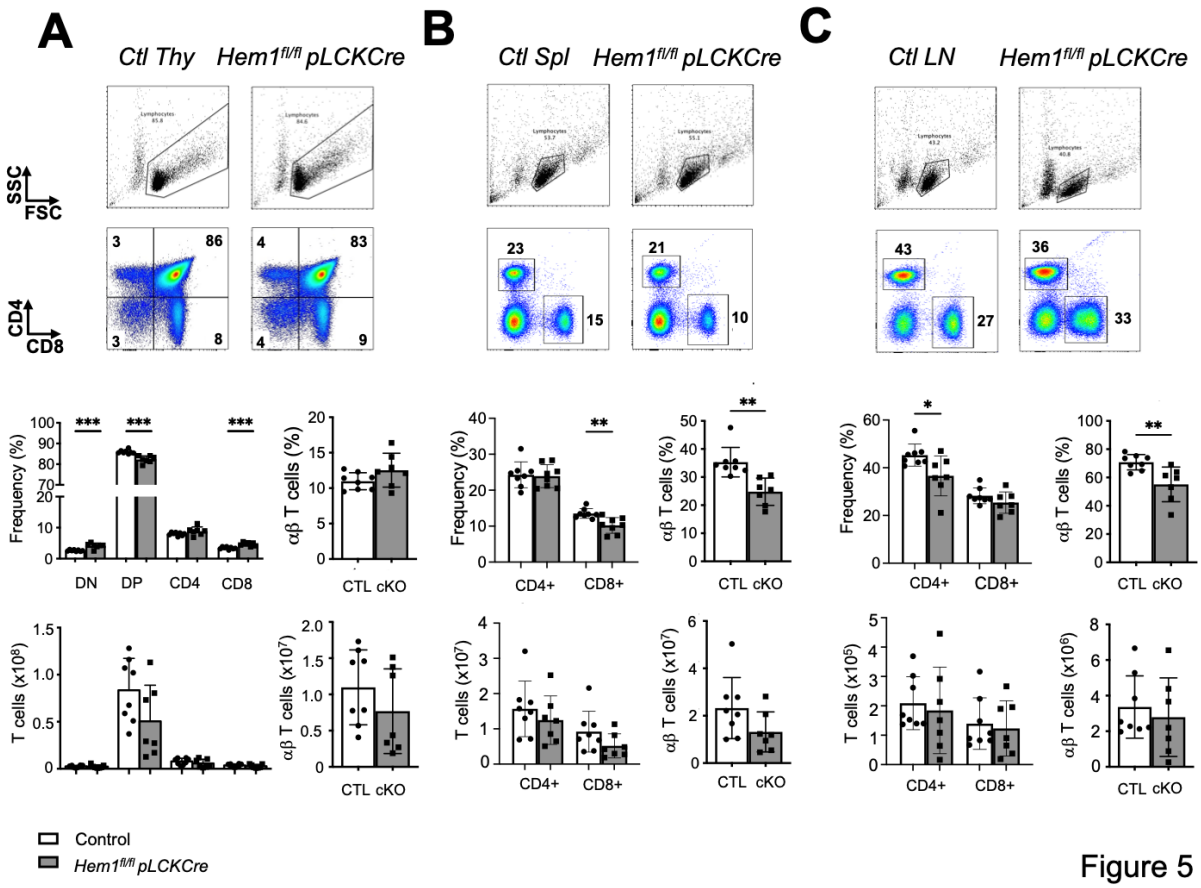

Figure 5

Figure 5. T cell-specific conditional deletion of *Hem1* disrupts T cell development. Total thymocytes, splenocytes, and lymphocytes from the axial and inguinal lymph nodes were isolated from *Hem1$^{fl/fl}$pLckCre* mice and *Hem1$^{fl/fl}$* littermate controls. T cell populations were analyzed by flow cytometry. **(A)** Representative flow cytometric dot plot histograms of thymocytes (top). Bar graphs and quantification of double negative (DN), double positive (DP), CD4$^+$CD8$^-$ (CD4), and CD8$^+$CD4$^-$ (CD8) cells in the thymus (bottom). **(B)** Representative flow cytometric dot plot histograms of splenocytes (top). Bar graphs and quantification of CD4$^+$ and CD8$^+$ T cells (bottom). **(C)** Representative flow cytometric dot plot histograms of cells from the axillary and inguinal lymph nodes combined (top). Bar graphs and quantification of CD4$^+$ and CD8$^+$ T cells (bottom). 10-12-week-old mice, n=7-8/group, each data point represents an individual mouse. Data are representative of 2 or more independent experiments. Bar graphs represent mean ± SD and were analyzed via unpaired Student's t test. *$P < 0.05$, **$P < 0.01$, ***$P < 0.001$.

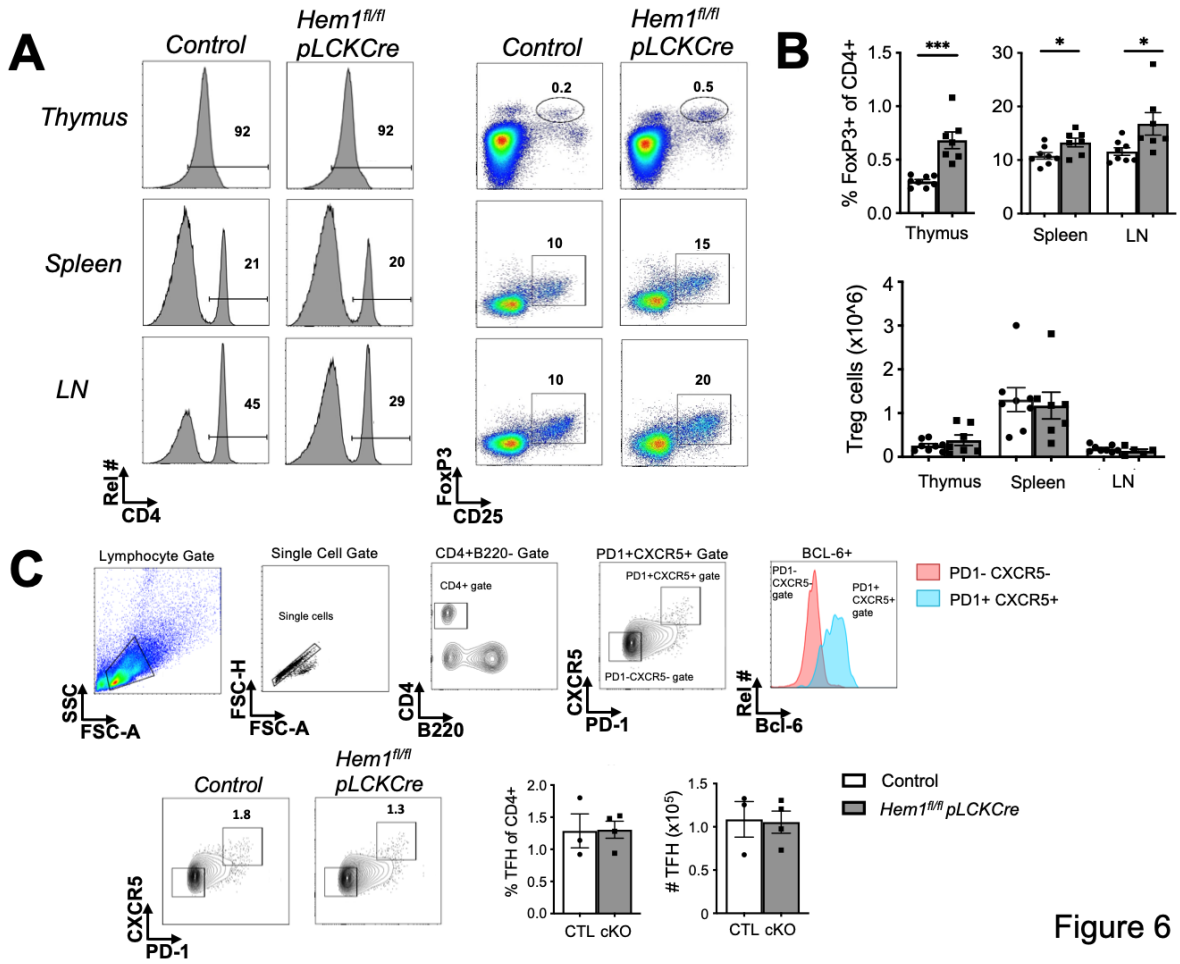

Figure 6. Mice with T cell-specific conditional deletion of *Hem1* have increased proportions of regulatory T cells, with no change in T follicular helper cells.

(A) Total thymocytes, splenocytes, and cells from axial and inguinal lymph nodes were isolated from *Hem1*$^{fl/fl}$*pLckCre* mice and *Hem1*$^{fl/fl}$ littermate controls. Representative flow cytometric dot plot histograms of gating strategy for Tregs. **(B)** Bar graphs and quantification of Treg cells ($CD4^+CD25^+FoxP3^+$). 10–12-week-old mice, n=7-8/group, data representative of 2 or more independent experiments. **(C)** Total splenocytes were isolated from *Hem1*$^{fl/fl}$*pLckCre* mice and *Hem1*$^{fl/fl}$ littermate controls. Representative flow cytometric dot plot histograms with gating strategy for T follicular helper cells. **(B)** Bar graphs and quantification of TFH cells ($CD4^+CXCR5^+PD\text{-}1^+$). 10-13-week-old mice, n=3-4/group, each dot represents an individual mouse. Bar graphs represent mean ± SD and were analyzed via unpaired Student's t test. $*P < 0.05$, $**P < 0.01$, $***P < 0.001$. Treg = regulatory T; TFH = T follicular helper.

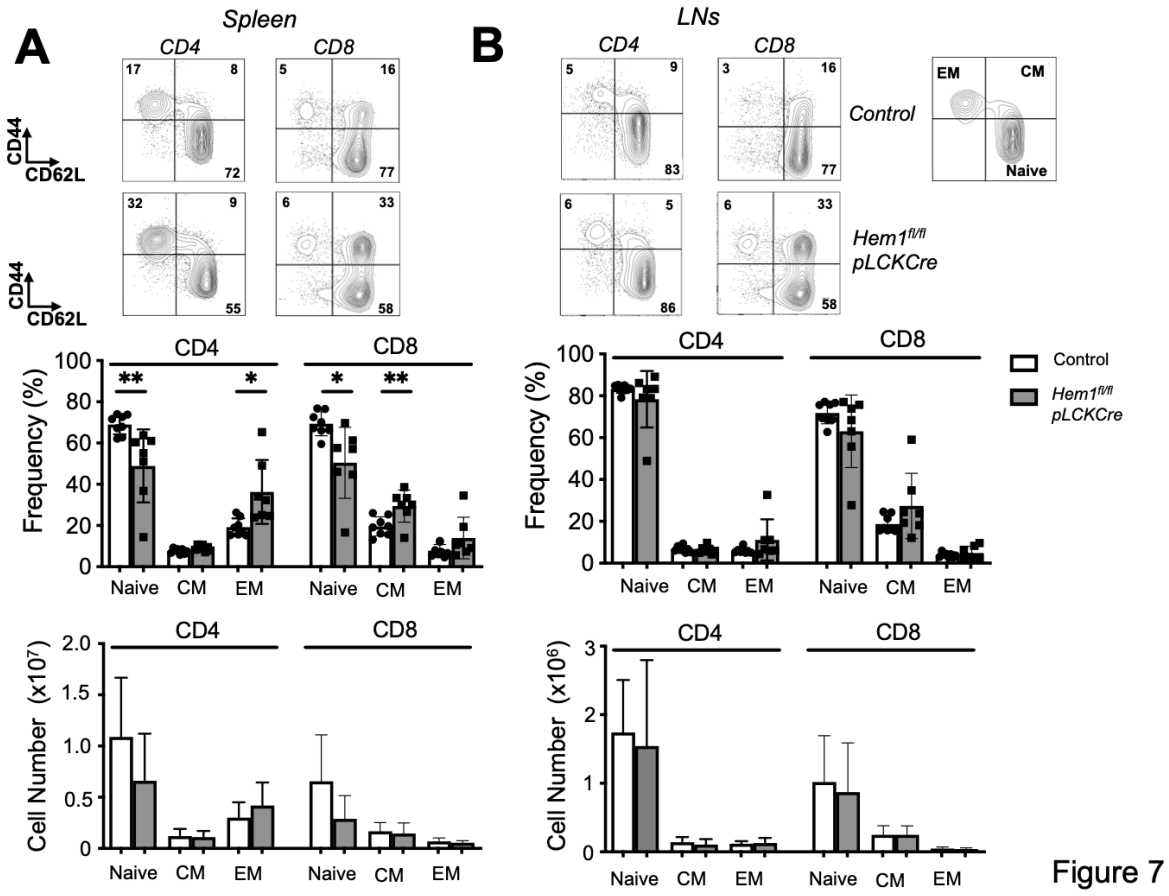

Figure 7. Conditional disruption of *Hem1* in T cells results in decreased frequency of naïve T cells with a concurrent increase in memory T cells in the spleen.

Total splenocytes and lymphocytes from the axial and inguinal lymph nodes were isolated from *Hem1*$^{fl/fl}$*pLckCre* mice and *Hem1*$^{fl/fl}$ littermate controls. T cell populations were analyzed by flow cytometry. **(A)** Representative flow cytometric dot plot histograms of splenocytes (top). Bar graphs and quantification of naïve (CD44^{-}CD62L^{+}), central memory (CD44^{+}CD62L^{+}), and effector memory (CD44^{+}CD62L^{-}) T cells from splenocytes (bottom). **(B)** Representative flow cytometric dot plot histograms (top) and bar graphs (bottom) of T cells harvested from lymph nodes. 10-12-week-old mice, n=7-8/group, data representative of 2 or more independent experiments, each dot represents an individual mouse. Bar graphs represent mean ± SD and were analyzed via unpaired Student's t test. *$P < 0.05$, ***$P < 0.001$. CM = central memory; EM = effector memory.

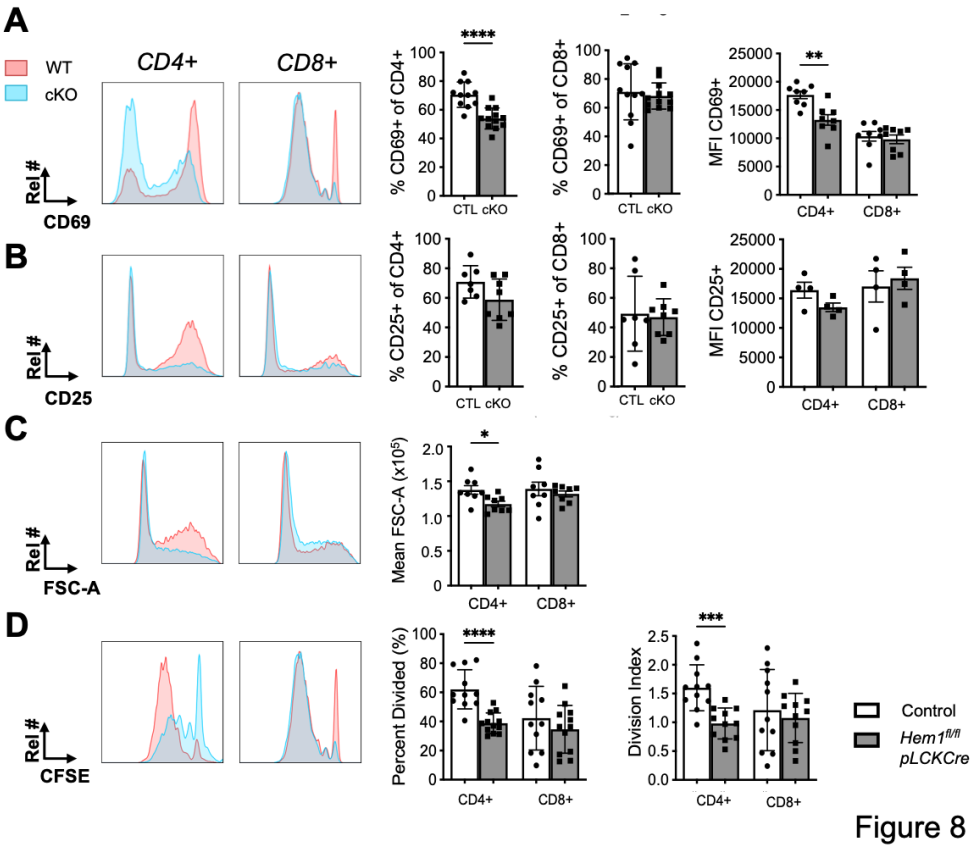

Figure 8

Figure 8. Conditional disruption of *Hem1* in T cells results in decreased CD4$^+$ T cell activation and proliferation with no changes in CD8$^+$ T cells.

Purified T cells from splenocytes harvested from *Hem1$^{fl/fl}$pLckCre* mice and *Hem1$^{fl/fl}$* littermate controls were stimulated with anti-CD3 and anti-CD28 antibodies. CD4$^+$ and CD8$^+$ T cell populations were analyzed by flow cytometry. Shown are **(A)** CD69 and **(B)** CD25 histograms (left), and bar graphs (right) representing the frequency and median fluorescence intensity (MFI) of CD69$^+$ and CD25$^+$ T cells after 24h of stimulation. **(C)** Forward scatter-A (FSC-A) histogram (left) and bar graphs representing mean FSC after 24h of stimulation (right). **(D)** Enriched T cells were stained with CFSE and then stimulated for 72h. Cell proliferation was assessed via flow cytometry showing CFSE histograms (left) and bar graphs of percent divided cells and the division index (right). 10-14-week-old mice, n=4-12/group, data representative of 2 or more independent experiments, each dot represents an individual mouse. Bar graphs represent mean ± SD and were analyzed via unpaired Student's t test. *$P < 0.05$, **$P < 0.01$, ***$P < 0.001$, ****$P < 0.0001$. Rel = Relative; CFSE = Carboxy Fluoroscein Succinimidyl Ester.

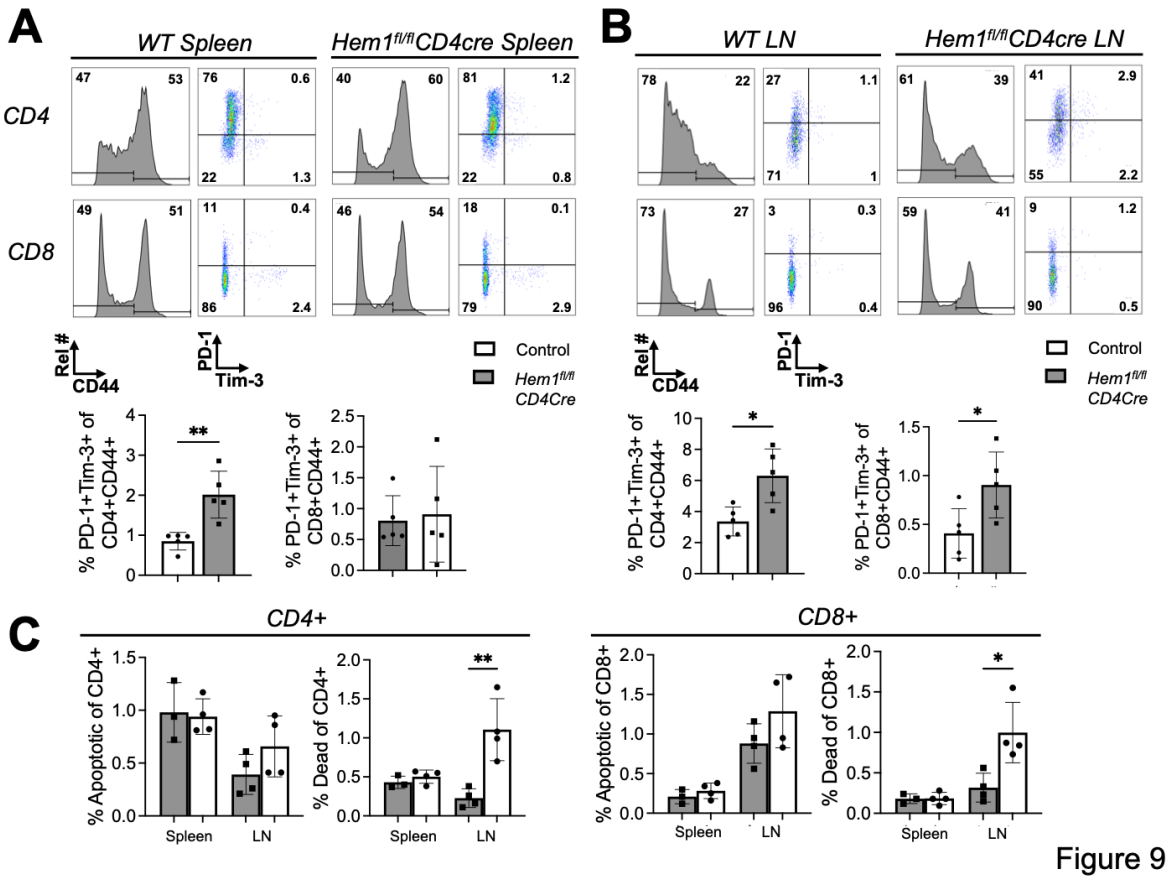

Figure 9

Figure 9. Increased T cell exhaustion and increased apoptosis in aged Hem1 deficient mice. Splenocytes and lymphocytes from the axial and inguinal lymph nodes were isolated from aged *Hem1*$^{fl/fl}$*CD4Cre* mice and *Hem1*$^{fl/fl}$ littermate controls. T cell populations were analyzed by flow cytometry. **(A)** Representative flow cytometric dot plot histograms showing the gating strategy for T cell exhaustion phenotype (CD44^{hi}PD-1+Tim-3+) for splenocytes (top). Bar graphs represent the frequency of T cells exhibiting an exhausted phenotype (bottom). **(B)** Representative flow cytometric dot plot histograms and bar graphs for T cells from lymph nodes. 52-weeks-old, n=3-4/group. Each dot represents an individual mouse. Two independent experiments performed (data from one experiment shown). Bar graphs represent mean ± SD and were analyzed via unpaired Student's t test. *$P < 0.05$, **$P < 0.01$, ***$P < 0.001$.

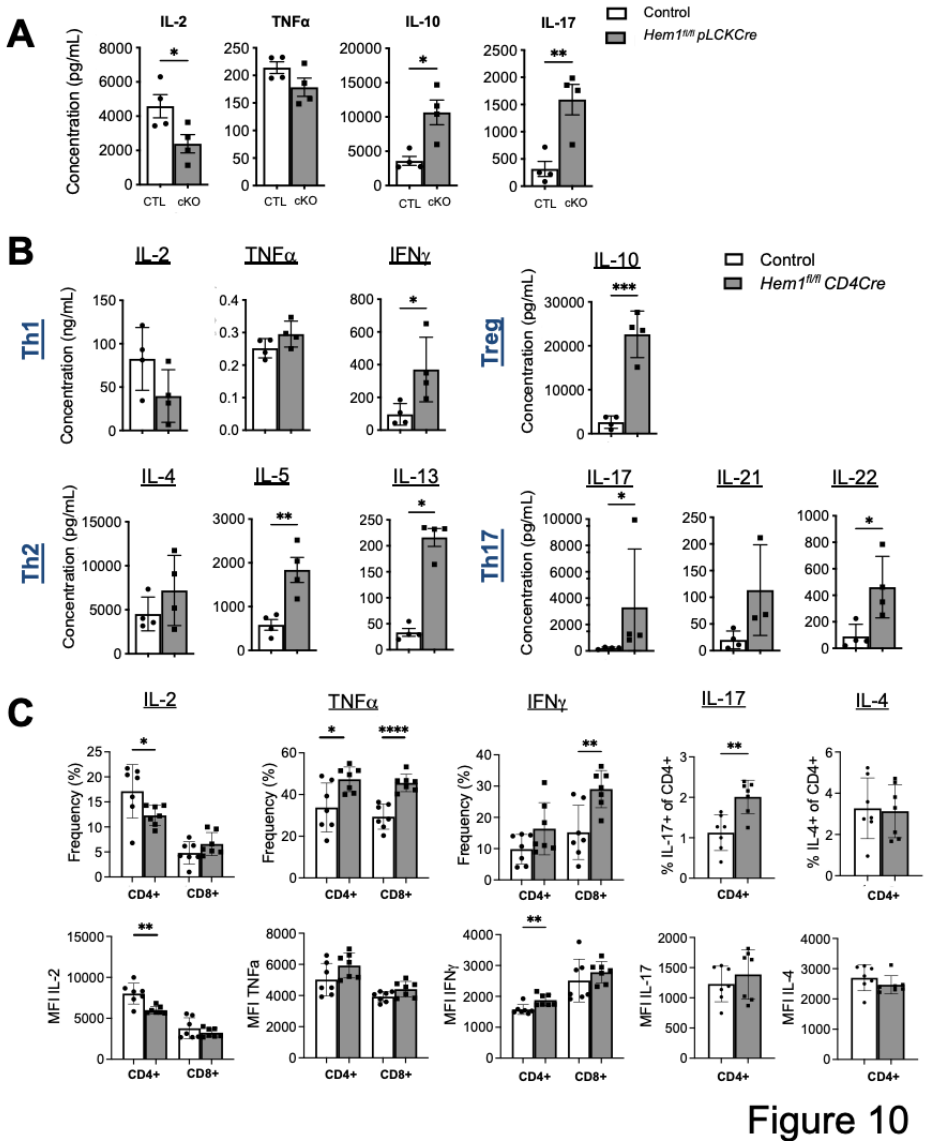

Figure 10. T cell-specific disruption of *Hem1* results in altered cytokine production.

(A) Purified pan T cells from splenocytes harvested from *Hem1*$^{fl/fl}$*pLckcre* mice and *Hem1*$^{fl/fl}$ littermate controls were stimulated with anti-CD3/antiCD28 antibodies for 72 hrs. Bar graphs represent concentrations of cytokines in supernatant measured by multiplex immunoassay. 10-13-week-old mice, n = 4/group. **(B)** Purified CD4^{+} T cells from splenocytes harvested from *Hem1*$^{fl/fl}$*CD4cre* mice and *Hem1*$^{fl/fl}$ littermate controls were stimulated with anti-CD3 and anti-CD28 antibodies for 72 hours. Bar graphs represent concentrations of cytokines in supernatant measured by multiplex immunoassay. Cytokines grouped by Th1 cells, Th2 cells, Th17 cells, and Treg production. 12-15-week-old mice, n=3-4/group. **(E)** Purified T cells from splenocytes harvested from *Hem1*$^{fl/fl}$*CD4cre* mice and *Hem1*$^{fl/fl}$ littermate controls were stimulated with anti-CD3 and anti-CD28 antibodies for 72 hours followed by a 5 hour stimulation with PMA and ionomycin. Cells were stained for intracellular cytokines (IL-2, TNFα, IFNγ,

IL-17, IL-4) and analyzed via flow cytometry. Bar graphs of frequency (top) and MFI (bottom) of cytokines. 11-15-week-old mice, n=7/group, data representative of 2 independent experiments, each dot represents an individual mouse. Bar graphs represent mean ± SD and were analyzed via unpaired Student's t test, IL-17 (C) was analyzed via Mann-Whitney test. $*P < 0.05$, $**P < 0.01$, $***P < 0.001$. MFI = median fluorescent intensity.

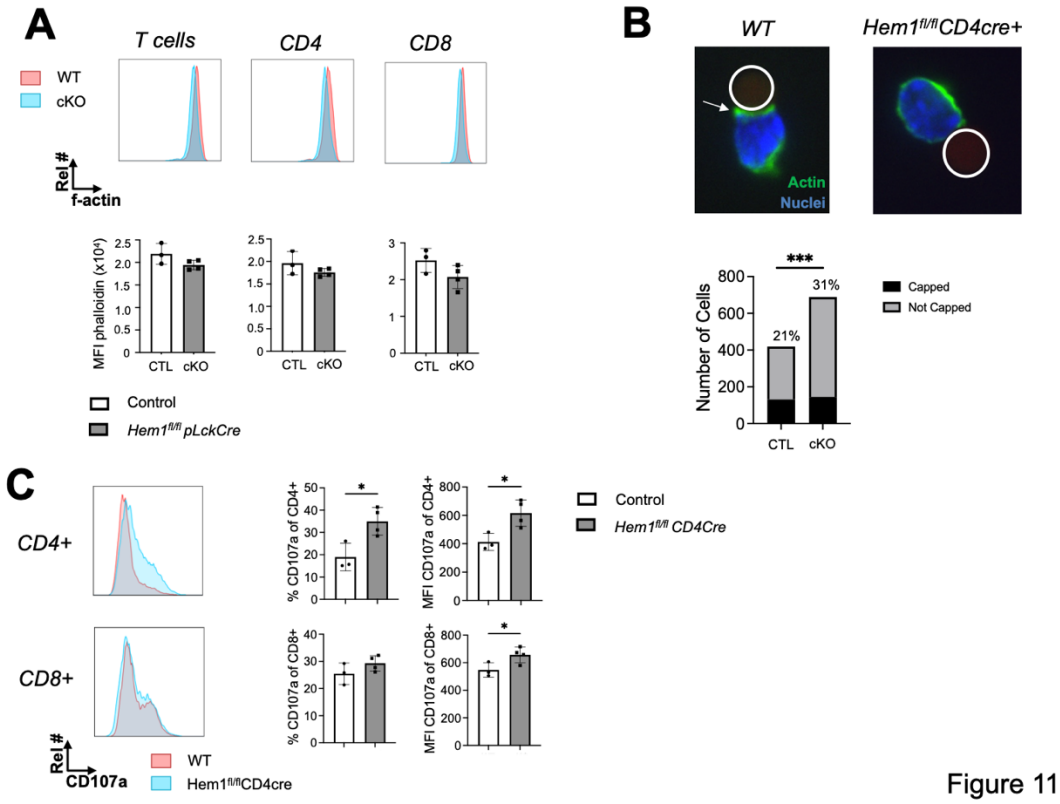

Figure 11

Figure 11. T cells specific disruption of *Hem1* results in defective f-actin polymerization, actin cap formation, and dysfunction of the cortical actin leading to increased exocytosis.

(A and B) T cells were purified from 10-14-week-old *Hem1$^{fl/fl}$pLckCre* mice and littermate controls. **(A)** T cells were stimulated with anti-CD3/anti-CD28 for 24 hrs, followed by stimulation with PMA/ionomycin for 15 minutes. T cell populations were analyzed by flow cytometry for actin staining. Representative flow cytometric histograms showing f-actin fluorescence (top), and bar graphs of MFI for actin. **(B)** Purified T cells were stimulated with anti-CD3/anti-CD28 Dynabeads at a 1:1 cell:bead ratio for 15 minutes. Cells were permeabilized and stained with ActinGreen 488 and NucBlue, and cytospin slides were prepared. Representative images captured at 100X using the Visitech VT-iSIM microscope, circle represents the bead, arrow represents the actin cap at the immune synapse (top). Bar graph represents the number of capped and not capped individual T cells, and percentage of capped cells is annotated. Fisher exact test used for statistical analysis of a 2x2 contingency table. **(C) E)** Splenocytes were harvested from 52-week-old *Hem1$^{fl/fl}$CD4Cre* mice and littermate controls and stimulated with PMA and ionomycin for 5 hours and CD107A surface localization assessed via flow cytometry. CD107A histograms (left) and bar graphs of frequency and MFI of CD107A$^+$ cells (right). Each dot represents an individual mouse, n=3-4/group. Bar graphs represent mean ± SD and were analyzed via unpaired Student's t test unless otherwise stated. *$P < 0.05$, ***$P < 0.001$.

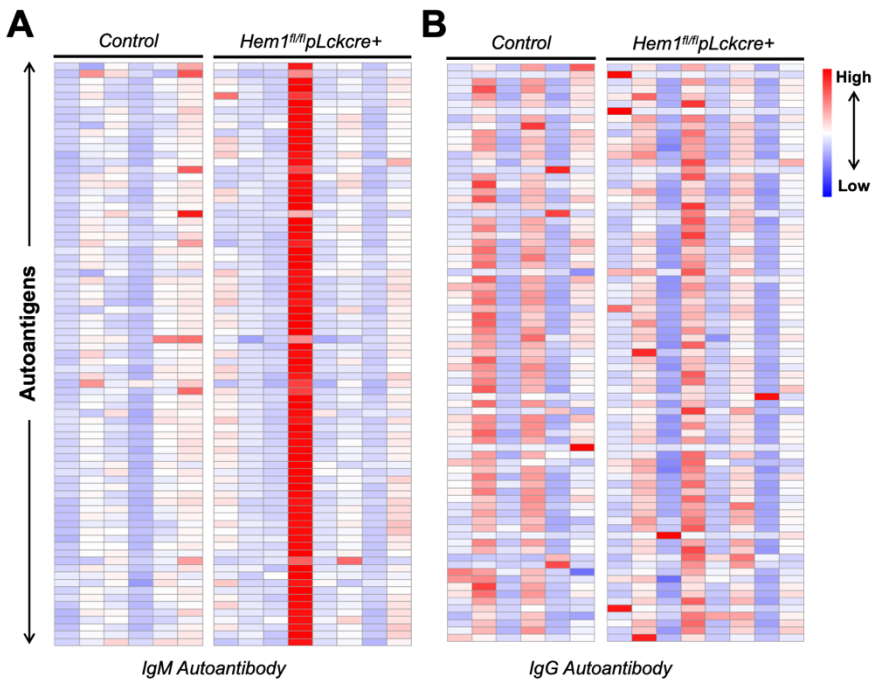

Figure 12

Figure 12. T cell specific disruption of Hem1 does not result in increased autoantibody formation

Sera were collected from female *Hem1*$^{fl/fl}$*pLckCre* and control mice ages 49–56 weeks (n=6-8/group). Sera were then hybridized to an autoantigen microarray containing 128 antigens. Shown are heatmaps depicting antigen reactivity (antibody score) for IgM **(A)** and IgG **(B)**.

REFERENCES

1. Avalos A, Tietsort JT, Suwankitwat N, Woods JD, Jackson SW, Christodoulou A, Morrill C, Liggitt HD, Zhu C, Li QZ, Bui KK, Park H, Iritani BM. Hem-1 regulates protective humoral immunity and limits autoantibody production in a B cell-specific manner. JCI Insight. 2022 May 9;7(9):e153597.
2. Badi YE, Pavel AB, Pavlidis S, Riley JH, Bates S, Kermani NZ, Knowles R, Kolmert J, Wheelock CE, Worsley S, Uddin M, Alving K, Bakke PS, Behndig A, Caruso M, Chanez P, Fleming LJ, Fowler SJ, Frey U, Howarth P, Horváth I, Krug N, Maitland-van der Zee AH, Montuschi P, Roberts G, Sanak M, Shaw DE, Singer F, Sterk PJ, Djukanovic R, Dahlen SE, Guo YK, Chung KF, Guttman-Yassky E, Adcock IM; U-BIOPRED Study Group. Mapping atopic dermatitis and anti-IL-22 response signatures to type 2-low severe neutrophilic asthma. J Allergy Clin Immunol. 2022 Jan;149(1):89-101.
3. Calvez R, Lafouresse F, De Meester J, Galy A, Valitutti S, Dupré L. The Wiskott-Aldrich syndrome protein permits assembly of a focused immunological synapse enabling sustained T-cell receptor signaling. Haematologica. 2011 Oct;96(10):1415-23.
4. Camargo LDN, Righetti RF, Aristóteles LRCRB, Dos Santos TM, de Souza FCR, Fukuzaki S, Cruz MM, Alonso-Vale MIC, Saraiva-Romanholo BM, Prado CM, Martins MA, Leick EA, Tibério IFLC. Effects of Anti-IL-17 on Inflammation, Remodeling, and Oxidative Stress in an Experimental Model of Asthma Exacerbated by LPS. Front Immunol. 2018 Jan 5;8:1835.
5. Camargo LDN, Dos Santos TM, de Andrade FCP, Fukuzaki S, Dos Santos Lopes FDTQ, de Arruda Martins M, Prado CM, Leick EA, Righetti RF, Tibério IFLC. Bronchial Vascular Remodeling Is Attenuated by Anti-IL-17 in Asthmatic Responses Exacerbated by LPS. Front Pharmacol. 2020 Sep 4;11:1269.
6. Castro CN, Rosenzwajg M, Carapito R, Shahrooei M, Konantz M, Khan A, Miao Z, Groß M, Tranchant T, Radosavljevic M, Paul N, Stemmelen T, Pitoiset F, Hirschler A, Nespola B, Molitor A, Rolli V, Pichot A, Faletti LE, Rinaldi B, Friant S, Mednikov M, Karauzum H, Aman MJ, Carapito C, Lengerke C, Ziaee V, Eyaid W, Ehl S, Alroqi F, Parvaneh N, Bahram S. NCKAP1L defects lead to a novel syndrome combining

immunodeficiency, lymphoproliferation, and hyperinflammation. J Exp Med. 2020 Dec 7;217(12):e20192275.

7. Chan MM, Wooden JM, Tsang M, Gilligan DM, Hirenallur-S DK, Finney GL, Rynes E, Maccoss M, Ramirez JA, Park H, Iritani BM. Hematopoietic protein-1 regulates the actin membrane skeleton and membrane stability in murine erythrocytes. PLoS One. 2013 8(2):e54902.
8. Chesné J, Braza F, Mahay G, Brouard S, Aronica M, Magnan A. IL-17 in severe asthma. Where do we stand? Am J Respir Crit Care Med. 2014 Nov 15;190(10):1094-101.
9. Cook SA, Comrie WA, Poli MC, Similuk M, Oler AJ, Faruqi AJ, Kuhns DB, Yang S, Vargas-Hernández A, Carisey AF, Fournier B, Anderson DE, Price S, Smelkinson M, Abou Chahla W, Forbes LR, Mace EM, Cao TN, Coban-Akdemir ZH, Jhangiani SN, Muzny DM, Gibbs RA, Lupski JR, Orange JS, Cuvelier GDE, Al Hassani M, Al Kaabi N, Al Yafei Z, Jyonouchi S, Raje N, Caldwell JW, Huang Y, Burkhardt JK, Latour S, Chen B, ElGhazali G, Rao VK, Chinn IK, Lenardo MJ. HEM1 deficiency disrupts mTORC2 and F-actin control in inherited immunodysregulatory disease. Science. 2020 Jul 10;369(6500):202-207.
10. Diz-Muñoz A, Thurley K, Chintamen S, Altschuler SJ, Wu LF, Fletcher DA, Weiner OD. Membrane Tension Acts Through PLD2 and mTORC2 to Limit Actin Network Assembly During Neutrophil Migration. PLoS Biol. 2016 Jun 9;14(6):e1002474.
11. Dupré L, Boztug K, Pfajfer L. Actin dynamics at the T cell synapse as revealed by immune-related actinopathies. Front Cell Dev Biol. 2021 9:665519.
12. Fontenot, J. D., Gavin, M. A. and Rudensky, A. Y. Foxp3 programs the development and function of $CD4^{+}CD25^{+}$ regulatory T cells. *Nat. Immunol.* 2003 4: 330–336.
13. Fujino S, Andoh A, Bamba S, Ogawa A, Hata K, Araki Y, Bamba T, Fujiyama Y. Increased expression of interleukin 17 in inflammatory bowel disease. Gut. 2003 Jan;52(1):65-70.
14. Gensous N, Charrier M, Duluc D, Contin-Bordes C, Truchetet ME, Lazaro E, Duffau P, Blanco P, Richez C. T Follicular Helper Cells in Autoimmune Disorders. Front Immunol. 2018 Jul 17;9:1637.

15. Hennet T, Hagen FK, Tabak LA, Marth JD. T-cell-specific deletion of a polypeptide N-acetylgalactosaminyl-transferase gene by site-directed recombination. Proc Natl Acad Sci U S A. 1995 Dec 19;92(26):12070-4.
16. Hofmann MA, Fluhr JW, Ruwwe-Glösenkamp C, Stevanovic K, Bergmann KC, Zuberbier T. Role of IL-17 in atopy-A systematic review. Clin Transl Allergy. 2021 Aug 13;11(6):e12047.
17. Hori, S., Nomura, T. and Sakaguchi, S., Control of regulatory T cell development by the transcription factor Foxp3. Science. 2003 299: 1057–1061.
18. Khattri, R., Cox, T., Yasayko, S. A. and Ramsdell, F. An essential role for Scurfin in $CD4^+CD25^+$ T regulatory cells. *Nat. Immunol.* 2003. 4: 337–342.
19. Kuwabara T, Ishikawa F, Kondo M, Kakiuchi T. The role of IL-17 and related cytokines in inflammatory autoimmune diseases. Mediators Inflamm. 2017 Feb 2017; 2017: 3908061.
20. Lee PP, Fitzpatrick DR, Beard C, Jessup HK, Lehar S, Makar KW, Pérez-Melgosa M, Sweetser MT, Schlissel MS, Nguyen S, Cherry SR, Tsai JH, Tucker SM, Weaver WM, Kelso A, Jaenisch R, Wilson CB. A critical role for Dnmt1 and DNA methylation in T cell development, function, and survival. Immunity. 2001 Nov;15(5):763-74.
21. Liang L, Hur J, Kang JY, Rhee CK, Kim YK, Lee SY. Effect of the anti-IL-17 antibody on allergic inflammation in an obesity-related asthma model. Korean J Intern Med. 2018 Nov;33(6):1210-1223.
22. Liu M, Zhang J, Pinder BD, Liu Q, Wang D, Yao H, Gao Y, Toker A, Gao J, Peterson A, Qu J, Siminovitch KA. WAVE2 suppresses mTOR activation to maintain T cell homeostasis and prevent autoimmunity. Science. 2021 Mar 26;371(6536):eaaz4544.
23. Nutthakarn Suwankitwat, Stephen Libby, H. Denny Liggitt, Alan Avalos, Alanna Ruddell, Jason W. Rosch, Heon Park, Brian M. Iritani; The actin-regulatory protein Hem-1 is essential for alveolar macrophage development. *J Exp Med* 5 April 2021 218(4): e20200472.
24. Mills, K.H.G. IL-17 and IL-17-producing cells in protection versus pathology. *Nat Rev Immunol* 2023 23:38–54.
25. Park H, Staehling-Hampton K, Appleby MW, Brunkow ME, Habib T, Zhang Y, Ramsdell F, Liggitt HD, Freie B, Tsang M, Carlson G, Friend S, Frevert C, Iritani BM. A

point mutation in the murine Hem1 gene reveals an essential role for Hematopoietic protein 1 in lymphopoiesis and innate immunity. J Exp Med. 2008 Nov 24;205(12):2899-913.

26. Park, H., Chan, M. M., & Iritani, B. M. Hem-1: putting the "WAVE" into actin polymerization during an immune response. *FEBS letters* 2010 584(24), 4923–4932.
27. Peters LA, Perrigoue J, Mortha A, Iuga A, Song WM, Neiman EM, Llewellyn SR, Di Narzo A, Kidd BA, Telesco SE, Zhao Y, Stojmirovic A, Sendecki J, Shameer K, Miotto R, Losic B, Shah H, Lee E, Wang M, Faith JJ, Kasarskis A, Brodmerkel C, Curran M, Das A, Friedman JR, Fukui Y, Humphrey MB, Iritani BM, Sibinga N, Tarrant TK, Argmann C, Hao K, Roussos P, Zhu J, Zhang B, Dobrin R, Mayer LF, Schadt EE. A functional genomics predictive network model identifies regulators of inflammatory bowel disease. Nat Genet. 2017 Oct;49(10):1437-1449.
28. Ricciardolo FLM, Sorbello V, Folino A, Gallo F, Massaglia GM, Favatà G, Conticello S, Vallese D, Gani F, Malerba M, Folkerts G, Rolla G, Profita M, Mauad T, Di Stefano A, Ciprandi G. Identification of IL-17F/frequent exacerbator endotype in asthma. J Allergy Clin Immunol. 2017 Aug;140(2):395-406.
29. Roberts AD, Ely KH, Woodland DL. Differential contributions of central and effector memory T cells to recall responses. J Exp Med. 2005 Jul 4;202(1):123-33. doi: 10.1084/jem.20050137.
30. Salzer E, Zoghi S, Kiss MG, Kage F, Rashkova C, Stahnke S, Haimel M, Platzer R, Caldera M, Ardy RC, Hoeger B, Block J, Medgyesi D, Sin C, Shahkarami S, Kain R, Ziaee V, Hammerl P, Bock C, Menche J, Dupré L, Huppa JB, Sixt M, Lomakin A, Rottner K, Binder CJ, Stradal TEB, Rezaei N, Boztug K. The cytoskeletal regulator HEM1 governs B cell development and prevents autoimmunity. Sci Immunol. 2020 Jul 10;5(49):eabc3979.
31. Sellers RS, Morton D, Michael B, Roome N, Johnson JK, Yano BL, Perry R, Schafer K. Society of Toxicologic Pathology position paper: organ weight recommendations for toxicology studies. Toxicol Pathol. 2007;Aug;35(5):751-5.
32. Shearer WT, Malech HL, Puck JM. Primary immunodeficiency: meeting the challenges. J Allergy Clin Immunol. 2007. Oct;120(4):753-5.

33. Wang B, Zhao P, Zhou Y, Meng L, Zhu W, Jiang C, Wang L, Cai Y, Lu S, Hou W. Increased expression of Th17 cytokines and interleukin-22 correlates with disease activity in pristane-induced arthritis in rats. PLoS One. 2017 Nov 28;12(11):e0188199.
34. Wu, J., Zhong, W., Yin, Y. *et al.* Primary immunodeficiency disease: a retrospective study of 112 Chinese children in a single tertiary care center. *BMC Pediatr*. 2009 19:410.
35. Zhu J, Cao Y, Li K, Wang Z, Zuo P, Xiong W, Xu Y, Xiong S. Increased expression of aryl hydrocarbon receptor and interleukin 22 in patients with allergic asthma. Asian Pac J Allergy Immunol. 2011 Sep;29(3):266-72.